2019

Modulation of Coxsackievirus Protease Activity by Polyamines

Courtney Noelle Dial

LOYOLA UNIVERSITY CHICAGO

MODULATION OF COXSACKIEVIRUS PROTEASE ACTIVITY BY POLYAMINES

A THESIS SUBMITTED TO

THE FACULTY OF THE GRADUATE SCHOOL

IN CANDIDACY FOR THE DEGREE OF

MASTER OF SCIENCE

PROGRAM IN INFECTIOUS DISEASE AND IMMUNOLOGY

BY

COURTNEY NOELLE DIAL

CHICAGO, ILLINOIS

AUGUST 2019

ACKNOWLEDGMENTS

First and foremost, I would like to thank my mentor, Dr. Bryan Mounce, PhD, for being supportive throughout the master's program as well as helping me through the daunting process of applying to PhD programs. I would also like to thank all of my lab mates, especially season 1 (Vince, Tom and Patrick), for being a huge support system throughout my time here. Lastly, I would also like to thank my undergraduate mentors: Dr. Jason J. Keleher, PhD, Dr. Sarah E. Powers, PhD and Dr. Simone Muench, PhD. Dr. Keleher and Dr. Powers were instrumental in teaching me basic laboratory research techniques as well as really lighting my passion for science. Dr. Muench, I only had for a short time while at Lewis, but I can honestly say she helped shape me into the woman I am today and for that I will be forever grateful.

Next, I would like to thank my committee, Dr. Edward Campbell, PhD, Dr. Gail Reid, MD, and Dr. Francis Alonzo III, PhD. For their constructive criticism and immense help in thinking about my project "a little deeper". I also wanted to give a special thank you to Dr. Alonzo, who agreed to be on my committee on extremely short notice. Lastly, I wanted to thank my original committee member Dr. Adam Driks, PhD, for help with my presentation skills and critical thinking and Dr. Susan Baker, PhD, for stepping in and helping on multiple parts of my project from the very beginning.

Lastly, the constant support from my friends and family has been critical throughout this process. The friends I made here were so important in that first semester of graduate school. My

family has always and will always support me in whatever I choose to do which I am extremely thankful for, even if they don't necessarily understand the complex science I am discussing. Most importantly I wanted to thank my grandparents, Jim and Carol Hopkins, my grandfather was always interested in science and I think is why I am interested in it as well, unfortunately he passed before I started undergrad, but I believe he would've been proud. My grandmother funded both my bachelor's degree as well as my master's degree. She was not able to see me finish or know that I have decided to get my PhD, but her support was the foundation for my education. Therefore, I would like to dedicate my thesis to both Jim and Carol Hopkins.

TABLE OF CONTENTS

LIST OF FIGURES

LIST OF TABLES

LIST OF ABBREVIATIONS

Coxsackievirus Type B	CVB3
Chikungunya Virus	CHIKV
Human Cytomegalovirus	CMV
Herpes Simplex Virus	HSV
Ornithine Decarboxylase 1	ODC1
Spermidine synthase	SRM
Spermine synthase	SMS
Spermidine/spermine acetyltransferase 1	SAT1
Polyamine oxidase	PAOX
Diflouromethylornithine	DFMO
Diethylnorspermidine	DENSpm
Virus Protein Genome Linked	VPg
Virion Protein	VP
Plaque Forming Unit	PFU
Melanoma Differentiation-Associated Protein 5	MDA5
Mitochondrial Antiviral Protein	MAVS
Zinc-Finger Antiviral Protein	ZAP
Eukaryotic Initiation Factor 4G	eIF4G
Death-Associated Protein 5	DAP5
Nuclear Factor Activated T-Cells 5	NFAT
Multiplicity of Infection	MOI

ABSTRACT

Coxsackievirus type B (CVB3) is one of the six serotypes of the Coxsackievirus family of non-enveloped, linear, and positive-sense single-stranded RNA viruses. It is a pathogenic enterovirus that belongs to the same genus as the notable pathogen poliovirus. CVB3 can cause a range of illnesses from a fever to gastrointestinal distress but is most noteworthy for the ability to cause viral myocarditis, a swelling of the heart muscle. Coxsackievirus, like all RNA viruses, tends to develop mutations rapidly due to its error prone polymerase and lack of proofreading activity. These mutations can be advantageous for the virus, allowing it to develop traits that enhance replication and pathogenesis. Due to its major clinical importance and a lack of available vaccine and antivirals, there is an impetus to identify effective antivirals against CVB3. In that regard, the virus' ability to mutate poses a major obstacle to successful antiviral treatment and must be explored further to better understand the mechanisms of antiviral resistance and improve drug development.

Polyamines are small positively charged molecules that are present in all cells and have crucial roles in processes such as transcription, translation, DNA replication and signaling. They are also fundamental to a virus' ability to infect a host. When drugs that diminish polyamines are added to cells, the virus' ability to replicate tapers. One drug that acts in this way is difluoromethylornithine (DFMO), which diminishes the production of polyamines by inhibiting the first step in polyamine synthesis: the conversion of ornithine to putrescine. In order to better understand how CVB3 could evolve resistance to antiviral treatments, CVB3 was serially

passaged in the presence of DFMO. The resultant mutations that arose in CVB3 may correlate with its ability to infect a host who is undergoing antiviral therapy.

Passaging CVB3 in the presence of DFMO illuminated 3 mutations: VP3 – 234R, which is a site in the viral capsid; 2A – Q29K and 3C- Q52R both of which are sites in viral proteases. These proteases are crucial for multiple stages of infection including protein processing and packaging. Due to the vital importance of the viral proteases, these mutations and their seeming tie with polyamines, the focus of this study will revolve around these mutations. From these initial findings, we hypothesize that polyamines modulate viral protease activity and CVB3 gains resistance to polyamine depletion via mutation of its protease(s).

CHAPTER ONE: BACKGROUND

Literature Review

Coxsackievirus Type B3 (CVB3)

Coxsackievirus Type B3 (CVB3) is a member of the *Picornaviridae* family of the *enterovirus* genus. Members of this family of viruses are non-enveloped and have a single stranded, positive sense RNA genome, and notable members include poliovirus and enterovirus 71[1,2]. CVB3, along with other enteroviruses, are spread via the fecal-oral route of transmission and can be found globally[1,3]. CVB3 infections occur frequently during the late summer months, as is the case with most enteroviruses [4]. It is thought that this is due to swimming being extremely common in the summer months and that CVB3 can survive in environmental conditions, especially warm water, for extended periods of time[5,6]. Although infection with CVB3 is relatively mild, the wide scope, its use as a model system, and its ability to cause severe disease makes it a virus worth studying.

Clinical Outcomes of CVB3

Typical CVB3 infections are self-limiting and typically present with a fever and gastrointestinal distress. However, CVB3 infection can progress to more serious conditions including myocarditis and endocarditis, Burnholm syndrome, and can also cause aseptic meningitis if the virus enters the central nervous system [2,7,8]. Myocarditis is an inflammation of the heart muscle which can either be caused by active viral replication, as the virus is able to persist in cardiac tissue[9], or from the immune response associated with clearing an active infection[9,10]. Myocarditis can lead to cardiomyopathy and cardiac failure which can result in permanent heart damage or even death[11,12]. Burnholm disease, also known as epidemic

pleurodynia, can cause chest and muscle pain. This presentation is associated with an active infection, which usually clears by itself, but can persist for up to 3 weeks [7,13]. Lastly, CVB3 is associated with aseptic meningitis, which is an inflammation of the meninges, a membrane covering the brain and spinal cord.

Epidemiologically, it is important to note is that CVB3, like all enteroviruses, spikes in the number of cases reported during the late summer months. Historically, this trend was also seen with poliovirus in the 1950s, presumably due to the increase in people swimming in infected water[4,6]. When considering how common CVB3 infection is, its ability to cause serious illness, and there being no current vaccine or antiviral treatment, novel antivirals are crucially needed in order to control infection.

Traditional Treatment of CVB3

Traditionally, due to a lack of vaccine or antivirals, CVB3 treatment is palliative. Typical treatment of CVB3, if symptoms are mild, include hydration and common over-the-counter cold medications. If an infection becomes more serious, such as myocarditis or aseptic meningitis, then the treatment is tailored to those conditions. In many cases myocarditis improves on its own, and treatment involves focusing on the symptoms[14]. If the myocarditis is serious, potentially including heart failure or arrhythmias, doctors will prescribe medication in order to reduce the chances of blood clots forming in the heart [15]. In more severe cases, an aggressive treatment regimen is followed such as inserting devices or balloon pumps [15]. In the case of aseptic meningitis, the illness normally clears on its own and standard viral care procedures are followed such as rest and hydration[16].

Polyamines and Cellular Functions

Polyamines are small positively charged molecules that are present in all cells. In eukaryotic cells there are three main polyamines, all produced by a single synthetic pathway [17,18]. In mammalian cells this pathway starts at ornithine which gets converted to putrescine via ornithine decarboxylase (ODC1), the rate limiting step in the polyamine synthesis pathway[17–20]. From there, putrescine is converted into spermidine by spermidine synthase (SRM) and spermidine is converted into spermine via spermine synthase (SMS). Spermidine and spermine can also go through extra metabolic processes by spermidine/spermine acetyltransferase 1 (SAT1) which adds an acetyl group to these polyamines, neutralizing the charge and marking them for export. Subsequently, acetylspermine and acetylspermidine can also go through polyamine oxidase (PAOX) action which converts spermine back to spermidine and spermidine back to putrescine[17,18,20]. This synthesis pathway is tightly regulated in cells, and is vitally important to overall cell health. A complete overview of the polyamine synthesis pathway can be seen in **Figure 1**[20]. Polyamines play roles in protein synthesis, membrane interactions, protein-RNA interactions, RNA structure and gene expression among other functions, making the process of polyamine synthesis crucial for virtually all steps in a cells lifecycle [17,18,21–24].

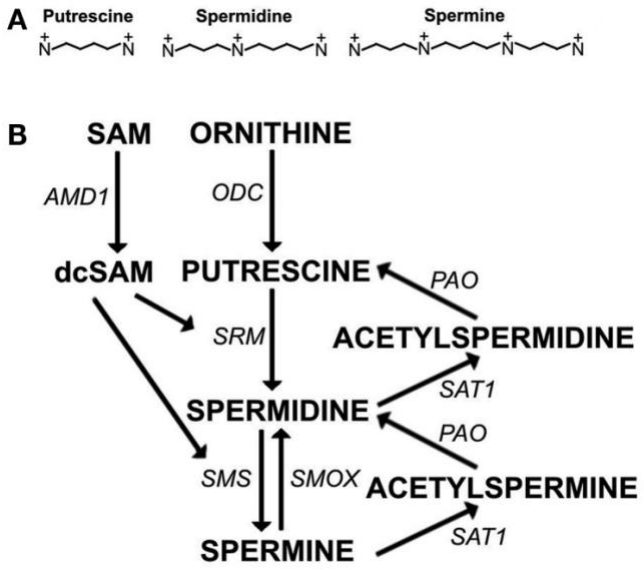

Figure 1. Polyamine Synthesis Pathway. Image adapted and modified from Wesley et. al. (2013)[20]. Permissions obtained from Wesley et. al.

Polyamines and Viral Infectivity

Not only are polyamines important for eukaryotic cells, they are also vital for viral infectivity[17]. Polyamines play multiple roles in the viral lifecycles, suggesting a crucial role in the virus' ability to infect a host [17]. Polyamines are important for genome packaging in DNA viruses, where viruses use polyamines to balance charge. [17,25–27] This has also been shown for RNA viruses. Polyamines are also important for DNA-dependent RNA polymerization in vaccinia virus and have been shown to impact DNA polymerase in herpes simplex virus (HSV) [17,28,29]. Genome replication as well as viral protein translation have also been shown to rely on polyamines in both RNA and DNA viruses [17,30,31]. Polyamine-depleting drugs on viruses such as chikungunya (CHIKV) have been shown as very potent, having effects on viral RNA polymerase, decreased overall viral translation and reduction in infectious virus produced [17,31,32]. Interestingly, vaccinia virus appears to stimulate polyamine synthesis upon infection, by upregulating ODC1 activity[17]. While polyamines have already been shown to be important for

DNA and RNA viruses, we are uncovering more functions for polyamines in viral replication rapidly [17,31–38].

DFMO and DENSpm

Due to the immense importance of polyamines in viral infectivity, blocking polyamine production can block viral infectivity. There are two drugs that can effectively block polyamine synthesis: difluoromethylornithine (DFMO) and N1,N11-diethylnorspermine (DENSpm). The former was originally developed as a cancer therapeutic and, has recently been repurposed as an FDA-approved treatment of trypanosomiasis or african sleeping sickness [39–42]. DFMO irreversibly binds to the active site of ODC1, which is the rate limiting enzyme in the polyamine synthesis pathway [17]. DENSpm, on the other hand, has a different mechanism of action. As a long carbon chain with a positive charge, DENSpm activates SAT1, depleting polyamines by neutralizing their charge and marking them for export [17]. Both of these drugs and how they affect the polyamine synthesis pathway can be seen in **Figure 2** below[17], where DFMO and DENSpm are boxed in red. DENSpm is also currently in clinical trials for cancer treatment and is shown to be an effective polyamine inhibitor [22]. In 2016, it was discovered that DFMO and DENSpm also have potent antiviral effects against a variety of RNA viruses[32]. These two drugs thus represent promising candidates in antiviral research and may be the sites of viral resistance development.

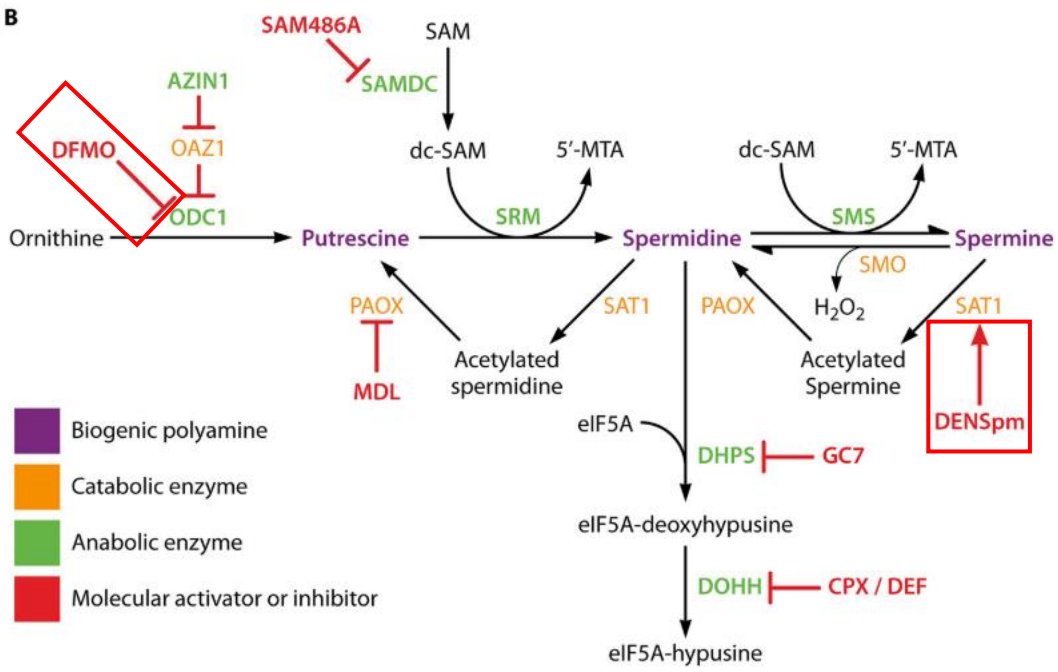

Figure 2. Polyamine Synthesis Pathway and Its Inhibitors. The complete polyamine synthesis pathway and its inhibitors. Specific inhibitors are boxed in red; those represent the drugs that we utilized throughout the course of this work. Image adapted and Modified from Mounce et. al. (2017)[17]. Permissions obtained from Mounce et. al.

RNA Virus Evolution

RNA viruses have a propensity to develop mutations along their genome with great ease, this is due to their error-prone RNA-dependent RNA polymerase and lack of proof-reading activity, meaning that RNA viral evolution can happen at an accelerated rate [43]. This susceptibility to mutations has been well documented in RNA viruses, and mutations can happen even through passaging in normal infection conditions[44–46]. Passaging involves successive rounds of viral infection in typically unfavorable condition, such as drug-treated cells or in a cell type a virus doesn't normally infect, where multiple rounds of passaging induces a virus has to adapt its genome in order to survive[47,48]. The mutations that may arise will give some indication as to what point in the viral life cycle these unfavorable conditions are affecting. Due to this

phenomenon, whenever a new antiviral is proposed it is important to know how a virus will adapt to this new condition.

Enterovirus Life Cycle

The basic lifecycle of enteroviruses is outlined below in **Figure 3** [1]. First, the virus binds to a cell, enters (viral uptake), and releases its RNA genome. The viral RNA is then translated into a large polyprotein which goes through proteolytic processing via proteases encoded in the genome [1]. In CVB3 this is mediated by the 2A ($2A^{pro}$) and 3C ($3C^{pro}$) proteases [1]. Once the polyprotein is cleaved into its main subunits, negative strand RNA synthesis occurs. This negative stranded RNA synthesis acts as a template for positive RNA strand synthesis. The CVB3 genome encodes a VPg (virus protein genome linked) that is covalently attached to the five-prime end of the positive stand RNA and acts as a primer during RNA synthesis, allowing VPg to facilitate this positive strand RNA synthesis [1,49]. When there is an abundant amount of positive stranded RNA, these genomes are encapsidated via the virion protein (VP) structural proteins. The cell then goes through cell lysis via viroporins and subsequent viral release [1,2,49,50]. As mentioned, polyamines play critical roles in these viral processes, but their exact mechanism of action, for RNA viruses, remains unclear. Therefore, if passaging techniques are utilized with DFMO as the drug condition, the potential mutations may give a better understanding as to how polyamines contribute to infectivity in the case of CVB3.

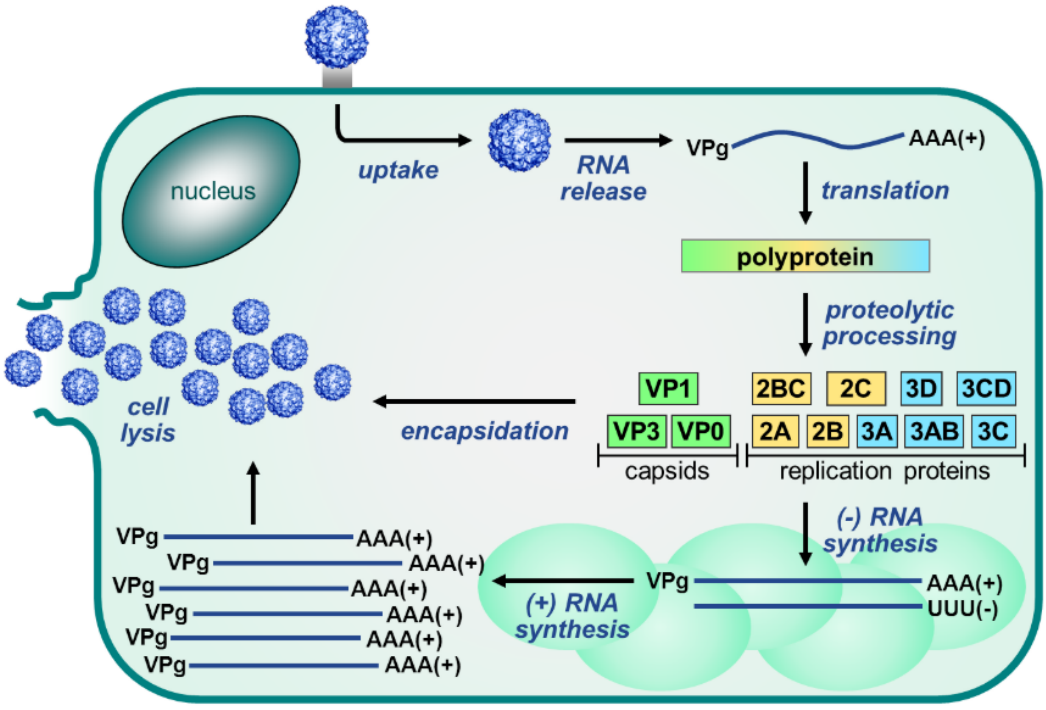

Figure 3. Coxsackievirus B3 Viral Life Cycle. Enterovirus life cycle diagram, beginning at viral binding and uptake through cell lysis and subsequent viral release. Image adapted and modified from van der Linden et. al. (2015) [1]. Permissions obtained from van der Linden et. al.

Enterovirus Genome Processing and Proteases

CVB3 proteases 2A ($2A^{pro}$) and 3C ($3C^{pro}$) are crucial for replication and infectivity, cleaving both viral and host proteins [1,51–59]. 2A facilitates the initial viral cleavage of the polyprotein, cleaving the P1 from the P2 protein segment [1], effectively separating the structural proteins from the replication proteins. The 3C protease is responsible for the bulk of the polyprotein cleavage events. These cleavage events are shown below in **Figure 4** [1]. Interestingly, 3C also acts as protease in a complex with 3D polymerase, called the 3CD polyprotein [60]. Although these proteases are vitally important in several infection cycle steps, the regulation of their activities and their overlapping and unique functions have yet to be fully elucidated. They are, however, important potential drug targets [61–63].

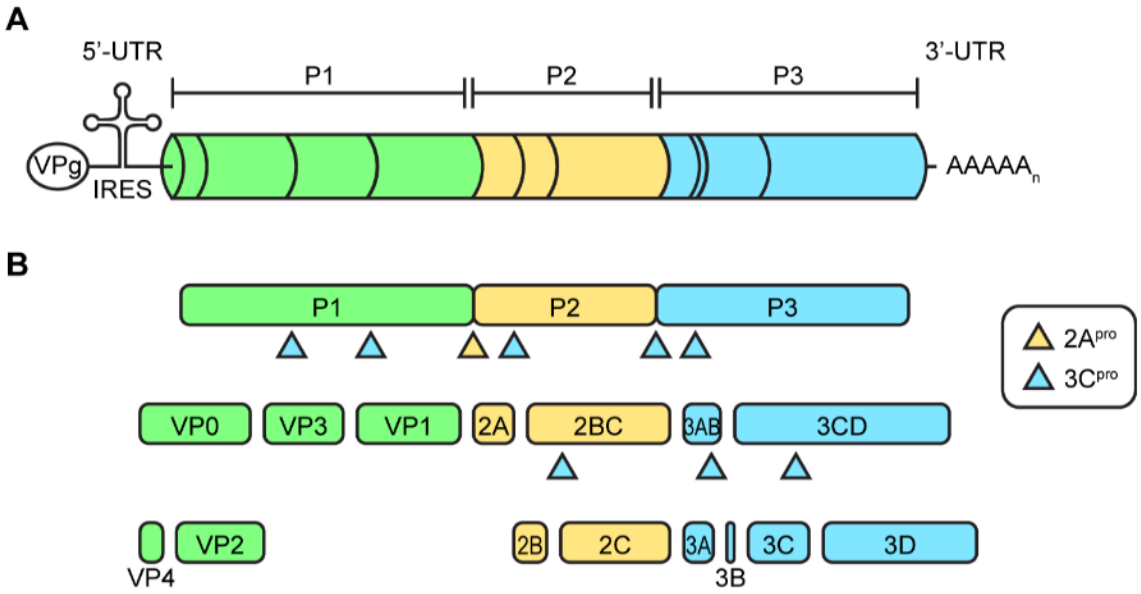

Figure 4. Proteolytic Processing of the 2A and 3C CVB3 Proteases. Viral proteolytic processing mediated by the 2A and 3C CVB3 proteases. Image adapted and modified from van der Linden et. al. (2015) [1]. Permissions obtained from van der Linden et. al.

The importance targeting these viral proteases in drug therapy is also highlighted by the protease's capacity to cleave several host proteins. This includes translation factors, immune effectors and signaling molecules. Both proteases cleave these factors in order to provide a proviral environment for effective viral infection. The known cellular targets include: MDA5, MAVS, eIF4G, DAP5, NFAT5 and zinc-finger antiviral protein [51–56]. Melanoma differentiation-associated protein 5 (MDA5) is a RIG-1-like receptor and has a pathogen- associated molecular pattern (PAMP) for dsRNA, which is specific to viral infections [51]. Along those lines the mitochondrial antiviral protein (MAVS) and zinc-finger antiviral proteins both act to inhibit viral replication [51,56]. The zinc-finger antiviral protein (ZAP) recruits cellular RNA degradation into the cytoplasm [55]. Eukaryotic initiation factor 4G (eIF4G) initiates translation; cleavage initiates translation shut-off [52,53,64]. Death-associated protein 5 (DAP5) is a translation initiation factor which mediates IRES- dependent translation [54]. Meaning that the viral cleavage of either eIF4G

or DAP5 would halt host cell translation. Lastly, nuclear factor activated T-cells 5 (NFAT5) is turned on in osmotic stress [55]. Cleavage of these proteins renders the cell unable to fight against viral infections and mount a productive immune response [55].

Aims and Hypothesis

Viral evolution, especially RNA viral evolution, can occur at an accelerated rate due to RNA virus' lack of proof-reading activity and error prone polymerase. This is the case for the positive sense single-stranded RNA virus, Coxsackievirus Type B (CVB3), a known public health threat. Previous work from our lab has shown that passaging CVB3 in polyamine-depleted conditions mutations occur in the protease regions of the CVB3 genome. Interestingly, there has never been an established link between polyamines and viral protease activity. Therefore, the overall hypothesis of this work is that CVB3 protease activity is modulated by polyamines and CVB3 gains resistance to polyamine depletion via mutation of its proteases. The goal of this project is to clarify the interaction occurring between polyamines and viral proteolytic activity through the following aims.

Our first aim is to fully characterize these mutants that resulted from previous passages of CVB3 in the presence of difluoromethylornithine (DFMO). Our goal here is to measure how CVB3 protease mutations affect viral fitness and resistance to other antivirals. We hypothesized that these mutations confer resistance to other polyamine depleting drugs, such as diethylnorspermidine (DENSpm), that these mutations are stable, and that their viral fitness may be altered due to the mutations.

Our second aim is to determine the effect of polyamines on protease activity. We hypothesize that polyamines play a direct role in modulating protease activity. Our goal is to

elucidate how polyamines contribute to CVB3 protease activity both utilizing a protease assay and monitoring a cellular cleavage event.

Our third aim is to investigate whether these mutants confer resistance to polyamine depletion via affecting protease activity. Our goal is to measure protease activity via Western Blot and protease assay and determine whether our protease mutants could cleave their targets in polyamine depleted conditions.

This work highlights the evolution of Coxsackievirus in the presence of novel antivirals, as well as the mechanistic features of the viral protease and ways in which clinicians can combat this resistance. In addition, we will clarify CVB3 protease functions and how it is modulated by polyamines.

CHAPTER TWO: MATERIALS AND METHODS

Cell Culture

Cells were maintained at 37^0C in 5% CO_2, in Dulbecco's modified Eagle's medium (DMEM; Life Technologies) with bovine serum and penicillin-streptomycin. The following reagent was obtained through BEI Resources, NIAID, NIH: Vero cells, Kidney (African green monkey), Expressing Luciferase (Luc2P), NR-10385 which were supplemented with 10% new-born calf serum (NBCS; Thermo-Fischer). HeLa and 293T cells, kindly provided by Dr. Ed Campbell, were supplemented with 10% fetal bovine serum (FBS; Thermo-Fischer).

Generation of CVB3 and 2A29K and 3C52R Mutants

CVB3 (Nancy strain)[65] was derived from the first passage of the virus in Vero cells after rescue from the infectious clone. Briefly, CVB3 infectious clone [66] was linearized with SapI (New England Biolabs [NEB]) and used to generate RNA in vitro (NEB). This RNA was transfected into Vero cells to recover the virus. The $2A^{29K}$ and $3C^{52R}$ mutant viruses were generated via site-directed mutagenesis of the wildtype CVB3 plasmid using the primers listed in Table 1 via mutagenic PCR with Phusion polymerase (Thermo-Fisher).

Table 1. Primers used in this study.

Protease/Target	Function	Sense	Sequence
2A	Clone	F	5'-GCTGCGGCCGCAGGCGCATTTGGACAACAATCAGG – 3'
	Clone	R	5'-GCTTCTAGATTACTGTTCCATTGCATCATCCTTCCAG- 3'
	Sequence	F	5'- CATGTCAAAGCGTGGATACCTAGAC - 3'
	Sequence	R	5'- GCACATGGGATTGGTATCTCCTGGG – 3'
	qPCR	F	5'- CATGTCAAAGCGTGGATACCTAGAC - 3'
	qPCR	R	5'- GCACATGGGATTGGTATCTCCTGGG – 3'
3C	Clone	F	5'-GTTGCGGCCGCTGGCCCTGCCTTTGAGTTCGCCG -3'
	Clone	R	5'-GCGTCTAGATTATTGCTCATCATTGAAGTAGTGTTTG -3'
	Sequence	F	5'- TATACAGGAGTGCCCAACCAGAAGC – 3'
	Sequence	R	5'- GAATGTACATGTTGGGAAACTTGCT – 3'
	qPCR	F	5'-AGGGCGAGATCAATCACATTAG-3'
	qPCR	R	5'-CTCTGCTGTTGCCTCACTATC-3'
2A ProTarget	Clone	F	5' – GATCCATGACCAACACCGGCGCGTTTGGCTAA – 3'
	Clone	R	5' – AGCTTTAGCCAAACGCGCCGGTGTTGGTCATG – 3'
3C ProTarget	Clone	F	5' – GATCCGCGATGGAACAGGGCTAA – 3'
	Clone	R	5'- AGCTTTAGCCCTGTTCCATCGCG – 3'
2A/3C ProTarget	Sequence	F	5'-GTAGTACAGACTGGAAAATATC-3'

Infection and Enumeration of Viral Titers

CVB3 (Nancy strain) [65] was derived from the first passage of virus in Vero cells (NR-10385), which were obtained through BEI Resources, National Institutes of Allergy and Infectious Diseases, National Institutes of Health (NR-10385). For all infections, DFMO and DENSpm

were maintained throughout infection as designated below. Viral stocks were maintained at -80^{0}C. For infection, virus was diluted in serum-free DMEM to a multiplicity of infection (MOI) of 0.1 on Vero cells, unless otherwise indicated. Viral inoculum was overlain on cells for 10 to 30 minutes, and the cells were washed with 1X PBS before replenishment of media. Supernatants were collected from CVB3 infected cells at 24 hpi and 48hpi. Dilutions of cell supernatant were prepared in serum-free DMEM and used to inoculate confluent monolayer of Vero cells for 10 to 15 min at 37^{0}C. Cells were overlain with 0.8% agarose in DMEM containing 2% NBCS. CVB3 samples incubated for 2 days at 37^{0}C. Following incubation, cells were fixed with 4% formalin and stained with crystal violet solution (10% crystal violet; Sigma-Aldrich). Plaques were enumerated and used to back-calculate the number of plaque forming units (pfu) per milliliter of collected volume.

Mutant CVB3 Propagation

Vero cells were treated with DFMO for four days prior to infection with CVB3 at MOI 0.1. After 24h, 1/10th of the cell culture volume was used to inoculate the next virus passage. This process was continued for ten passages, at which time RNA was purified from the cellular supernatant, reverse transcribed, amplified using CVB3-specific primers, and Sanger sequenced. Sequences were aligned to CVB3 parental genome and mutants were confirmed by manual chromatogram verification.

Drug Treatments

Difluoromethylornithine (DFMO; TargetMol) and N1,N11-Diethylnorspermine (DENSpm; Santa Cruz Biotechnology) were diluted to 100x concentrations (100mM and 10mM, respectively) in sterile PBS. For DFMO treatments, cells were trypsinized (Zymo Research) and reseeded with fresh medium supplemented with 2% serum to allow for reattachment. Following

overnight incubation, cells were treated with 100 µM, 500 µM, 1 mM, or 2 mM DFMO. Cells were incubated with DFMO for 96 hours to allow for depletion of polyamines. For DENSpm treatment, cells were treated with 100 nM, 1 µM, 10 µM, 100 µM, and 1mM concentrations fo 16 hours prior to infection. During CVB3 infection, media was collected and saved from the cells. The same medium containing DFMO and DENSpm was then used to replenish the cells following infection. Cells were incubated at the appropriate temperature for the duration of the infection.

DFMO and DENSpm Passages

Vero cells were treated with either 500µM DFMO or 100µM DENSpm, or left untreated, for 96 or 16hrs respectively. For the first passage, cells were infected at an MOI of 0.1, and supernatants were collected at 24hpi. For the blind passages, 50µL of supernatant was used to inoculate subsequent passages. For fixed-MOI passages, viral titers were determined, and the next passage was infected at an MOI of 0.1.

RNA purification and cDNA synthesis

Media was cleared from cells and Trizol reagent (Zymo Research) directly added. Lysate was then collected, and RNA was purified according to the manufacturer's protocol utilizing the Direct-zol RNA Miniprep Plus Kit (Zymo Research). Purified RNA was subsequently used for cDNA synthesis using High Capacity cDNA Reverse Transcription Kits (Thermo-Fischer), according to the manufacturer's protocol, with 10-100 ng of RNA and random hexamer primers.

DFMO and DENSpm Sensitivity Assays

Vero cells were treated with either 100µM to 2000µM DFMO for 4 days or 1µm to 100µM DENSpm for 16h prior to infection with CVB3 at an MOI of 0.1. At 24 hpi, supernatants were collected, and titers were determined via Vero cell plaque assay.

Stability and Fitness Assays

To measure stability of the mutations, Vero cells were infected at an MOI of 0.1 with all of the viral mutants for 24h. Virus was then passed to new cells by transferring 50µL supernatant. After five passages, RNA was extracted and purified from supernatants and reverse transcribed. Sanger sequencing was used to determine whether mutations were stable over the passages by looking at the chromatograms and determining presence or absence of the mutant nucleotide. Fitness assays were similarly performed, but Vero cells were infected at an MOI of 0.1 with an equal combination of wild-type and mutant CVB3 and passaged five times. Fitness was determined via Sanger sequencing and analysis of the chromatogram to determine if the wild-type or mutant nucleotide was most abundant in the sample.

Plaque Size Measurement

To quantify the relative plaque sizes of the different CVB3 mutants, Vero cells were seeded in 10 cm dishes and grown to confluence in 10% Fetal Bovine Serum and DMEM. Approximately 30 plaque-forming units (PFU) of each mutant was diluted in a 2.5 mL inoculum of serum-free DMEM. The media on the Vero cells was aspirated and replaced with the 2.5 mL inoculum containing the virus. The inoculum was incubated on the cells for approximately 30 min at 37 ◦C. After 30 min, an overlay of 8 mL 0.8% agarose was added to each dish. The dishes were incubated at 37 ◦C for 2 days to allow plaque formation. The cells were fixed with 4% formalin and the agarose plugs removed. The fixed cells were stained with crystal violet. Plaque size was determined using ImageJ software (Version 1.51k).[67]

Protease Plasmid Cloning

Primers were designed to target either the wild-type 2A or 3C protease in the CVB3 genome. CVB3 plasmids containing either the 2A mutant protease or 3C mutant protease were used to clone the mutant proteases. To target the 2A and 2A mutant proteases, the primers included SacI and XbaI recognition sites (Table 1). Primers against the 3C and 3C mutant proteases included NotI and XbaI recognition sites. Protease sequences were amplified via PCR and cloned into the pFLAG-CMV-LAP1 vector with either the restriction enzyme pair SacI/XbaI or NotI/XbaI for 2A and 3C respectively. Clones were verified by sequencing (GenScript). Oligonucleotide sequences corresponding to the amino acid sequence for the wild-type and mutant 2A and 3C protease targets were designed and cloned into the pGlo-3F vector and verified by sequencing (GenScript).

Transfections

293T cells were plated at 80%–90% confluency and either treated with 100 µM, 500 µM, 1000µM or 2000 µMDFMO for 4-days or left untreated. The plasmids were then transfected in the combinations described in the figures, according to the manufacturer's protocol, using LipoD293 (SignaGen Laboratories). The transfection was incubated at 37°C for 24h.

Luciferase Protease Assay

293T cells were treated with either 100µM, 500µm, 1000µm, or 2000µm DFMO for 4 days or left untreated. They were then transfected using LipoD293 (SignaGen Laboratories) with the 2A substrate alone, 3C substrate alone, 2A substrate plus the 2A WT protease or 2A mutant protease, or the 3C substrate plus the 3C WT protease or the 3C mutant protease. For luciferase assays, cells were combined with firefly (Bright-Glo; Promega) followed by subsequent Renilla (Stop and Glo; Promega) luciferase substrate 24h post-transfection. Luciferase assays were

performed according to the manufacturer's recommendations (Promega) and results were measured via the Veritas Microplate Luminometer (Turner BioSystems).

Western Blot

Samples were collected with Bolt LDS Buffer and Bolt Reducing Agent (Invitrogen) and run on polyacrylamide gels. Gels were transferred using the iBlot 2 Gel Transfer Device (Invitrogen). Membranes were probed with primary antibodies for eIF4G, (1:1000, Santa Cruz Biotechnology), GAPDH (1:1000, Santa Cruz Biotechnology), and β-actin (1:5000, Santa Cruz Biotechnology). Membranes were treated with SuperSignal West Pico PLUS Chemiluminescent Substrate (ThermoFisher Scientific) and visualized on ProteinSimple FluorChem E imager.

Statistical Analysis

Prism 6 (GraphPad) was used to generate graphs and perform statistical analysis. For all analyses, one-tailed Student's t test was used to compare groups, unless otherwise noted, with a $p = 0.05$. For tests of sample proportions, p values were derived from calculated Z scores with two tails and a $p = 0.05$.

CHAPTER THREE: RESULTS

Fixed Passages of CVB3

Previous fixed passages of CVB3 in the presence of DFMO resulted in 2 mutations in the protease region of CVB3. These passages were done in a controlled manner, infecting the subsequent cells with a multiplicity of infection (MOI) of 0.1 and increasing the concentration of drug with each subsequent passage (**Figure S1**). This method forces bottlenecking. It is also important to note that, along with the drug-treated condition, untreated cells were passaged with CVB3 in a similar manner. These untreated cells act as a control: if there are mutations in passaged virus from the nontreated conditions and the same mutations show up in our drug treated conditions, then it is reasonable to assume that those mutations are occurring due to the process of passaging, not as a result of the drug. Therefore, only mutations that occur in the drug treated conditions and not in the untreated conditions were considered for further investigation. At passage five, the virus was tested for its susceptibility to DFMO treatment. Vero cells were treated with increasing concentrations of DFMO and the percent replication of the virus was measured by dividing the samples by the NT control in their respective concentrations of DFMO. (**Figure S2**). The virus passaged in the presence of DFMO has a significantly higher percent replication rate. This is indicative of intrinsic resistance to DFMO treatment at passage five.The mutations we studied further were in the protease region of the CVB3 genome: Q29K in the 2A protease and Q52R in the 3C protease. We then cloned these mutations in the CVB3 parental

strain using mutagenic PCR. In addition to the $2A^{Q29K}$ and $3C^{Q52R}$ mutant, a $2A^{Q29K}3C^{Q52R}$ double mutant was also generated. After confirming the presence of these mutations, we generated infectious virus via transfection and measured virus titer by plaque assay over several rounds of replication, seen in **Figure 1**.

Assessing the Mutants Resistance to DFMO

To determine if these resultant CVB3 mutants were resistant to DFMO, Vero cells were treated with 500μM DFMO 4-days prior to CVB3 infection or left untreated, then infected at an MOI of 0.1 with wild-type CVB3 or mutant CVB3. The supernatant was collected from these cells over a time course and CVB3 titers were determined via viral plaque assay (**Figure 5**). All viruses in untreated conditions had similar growth kinetics even with the protease mutation. This is highlighted by the similar viral titers of the mutants to WT in NT condition (teal markers). In DFMO-treated cells the wild-type CVB3 exhibited significant reductions in titer, which persisted to 72hpi. When looking at the mutants vs the WT in DFMO treated conditions (orange markers) the protease mutants (either alone or in combination) exhibited a partial rescue in viral titer compared to the wild-type virus.

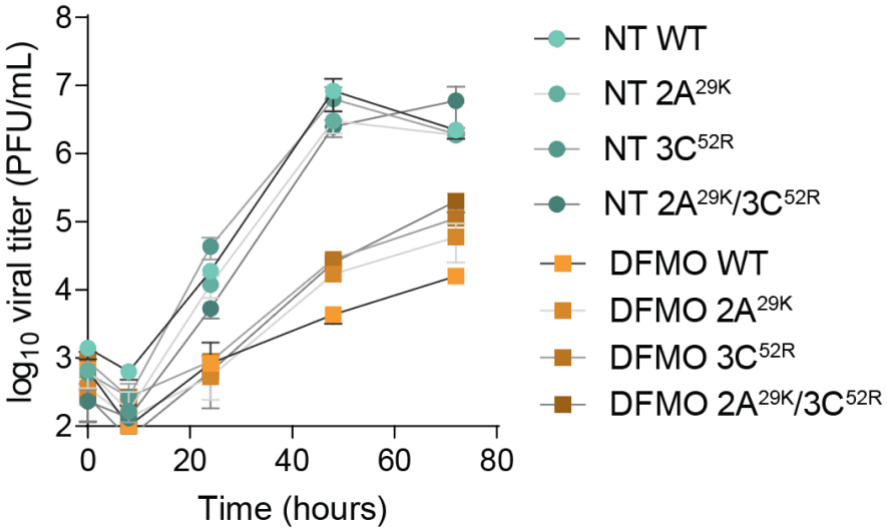

Figure 5. Growth Kinetics of Both the WT and Mutant Viruses in NT and DFMO Treated Conditions. Vero cells were either treated with DFMO for 4 days or left untreated, then infected at an MOI of 0.1 with either WT CVB3 or one of the mutant viruses. Growth kinetics were observed via viral titer from 16-72 hpi. Error bars represent ± 1 SEM

To quantify resistance, we measured viral titers of wild-type and the protease mutants in untreated and DFMO pre-treated conditions over a range of concentrations (**Figure 6**). Vero cells, in both the pre-treated and untreated conditions, were infected at an MOI of 0.1 and viral titers were measured at 24hpi. **Figure 6** displays that WT virus has significantly higher sensitivity to DFMO conditions (evident by the drop in viral titer) compared to the $2A^{Q29K}$, $3C^{Q52R}$, and the $2A^{Q29K}3C^{Q52R}$ mutants. These mutants exhibit partial resistance, indicated by the increased viral titers in DFMO-treated conditions. We then measured percent replication by dividing the titer in DFMO treatment conditions at 500µm by the titer in untreated conditions (**Figure 7**). We observed that all the mutants showed higher replication than that of the WT virus, suggesting that the mutant viruses could replicated better than WT in DFMO-treated conditions. Individually, the protease mutations showed similar levels of replication in these conditions.

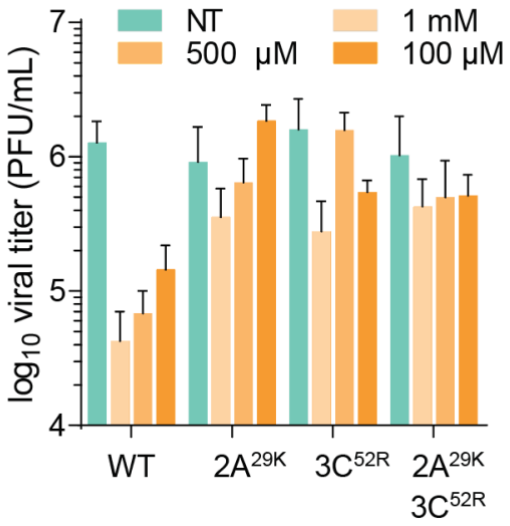

Figure 6. Testing the Mutants Susceptibility to DFMO Treatment. Vero cells were either treated with 500µM, 1mM or 5mM DFMO for 4d or left untreated. Cells were infected with the WT or mutant viruses at an MOI of 0.1, 24 hpi viral titers were enumerated. Error bars represent ± 1 SEM

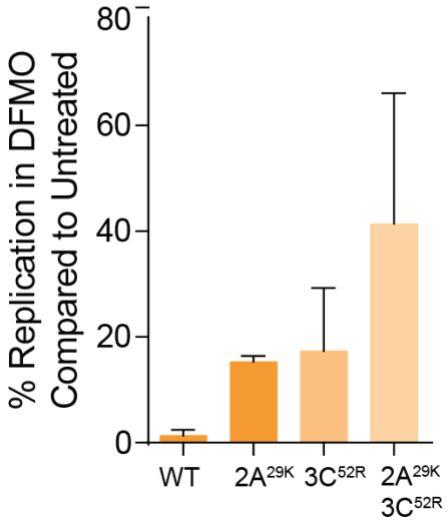

Figure 7. Determining the Percent Replication of the Mutants in DFMO Conditions Compared to WT. Vero cells were treated with 500µM DFMO and infected at an MOI of 0.1 with the WT or mutant viruses. At 24 hpi viral titers were enumerated. The results are the titers of each respective virus divided by the titer in untreated conditions. Error bars represent ± 1 SEM

Determining the Stability and Fitness of the Mutants

In order to determine the stability of these mutants, WT CVB3 as well as the $2A^{Q29K}$, $3C^{Q52R}$, and the $2A^{Q29K}3C^{Q52R}$ mutants were passaged on untreated Vero cells for five passages. At the end of the fifth passage, supernatants were collected, RNA was purified, reverse transcribed, and used for Sanger sequencing the mutations of interest (**Figures 8-10**). We found that all of the mutations were present after the fifth passage

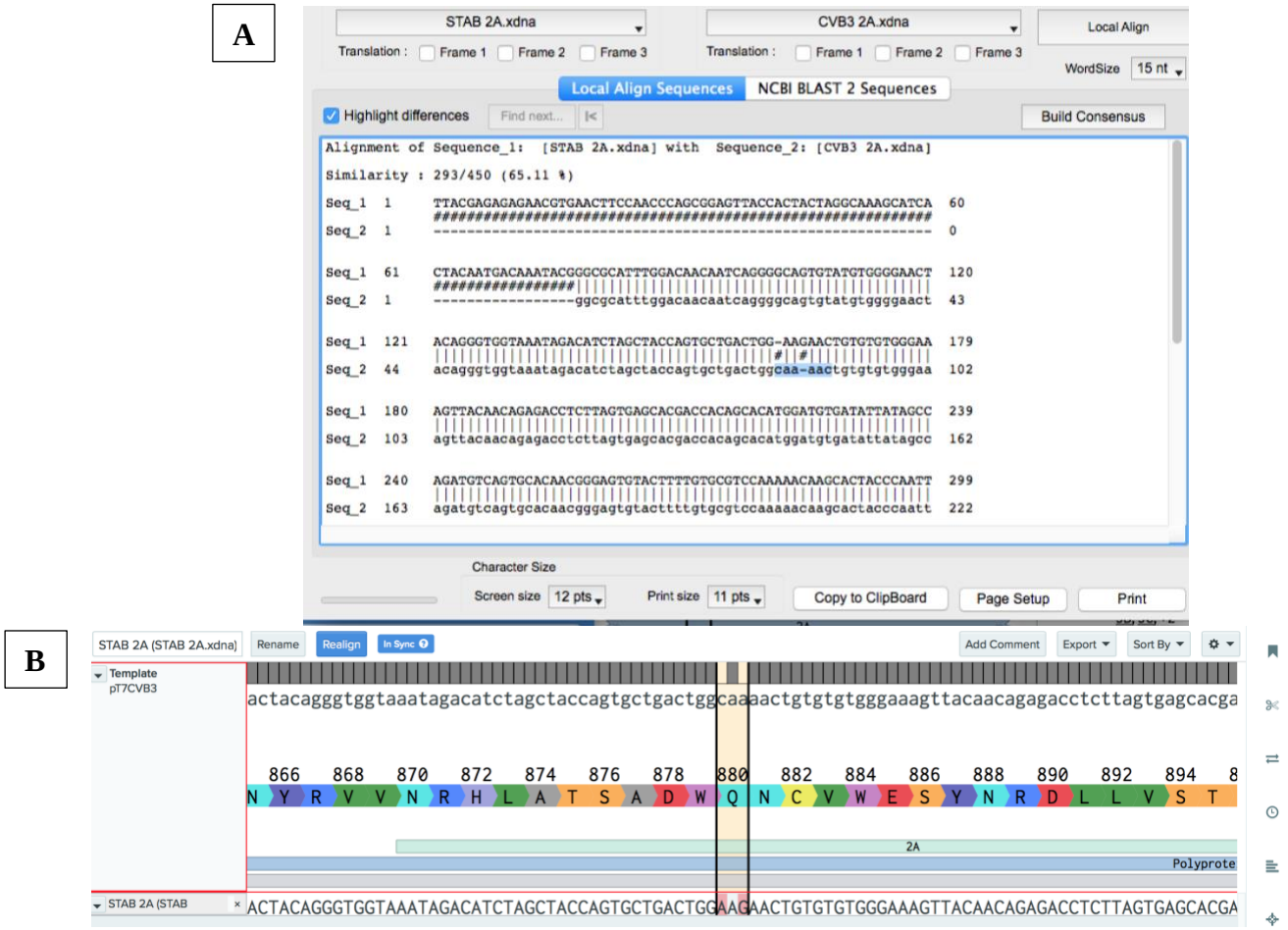

Figure 8. Analysis of the Stability of the $2A^{Q29K}$ mutant. The $2A^{Q29K}$ mutant was passaged in untreated Vero cells for a total of 5 passages, RNA was then extracted from the supernatant, purified, reverse transcribed than sent off for sequencing. A) Comparative look of the passaged $2A^{Q29K}$ mutant sequence aligned with the WT 2A sequence utilizing serial cloner. Octothorp (#) indicate differences in sequence. Highlighted sequence is the 2A mutation. B) Comparative look of the passaged $2A^{Q29K}$ mutant sequence aligned with the WT sequence utilizing Benchling software. Highlighted portion is the 2A mutation site. Red nucleotides indicate differences from WT sequence.

A

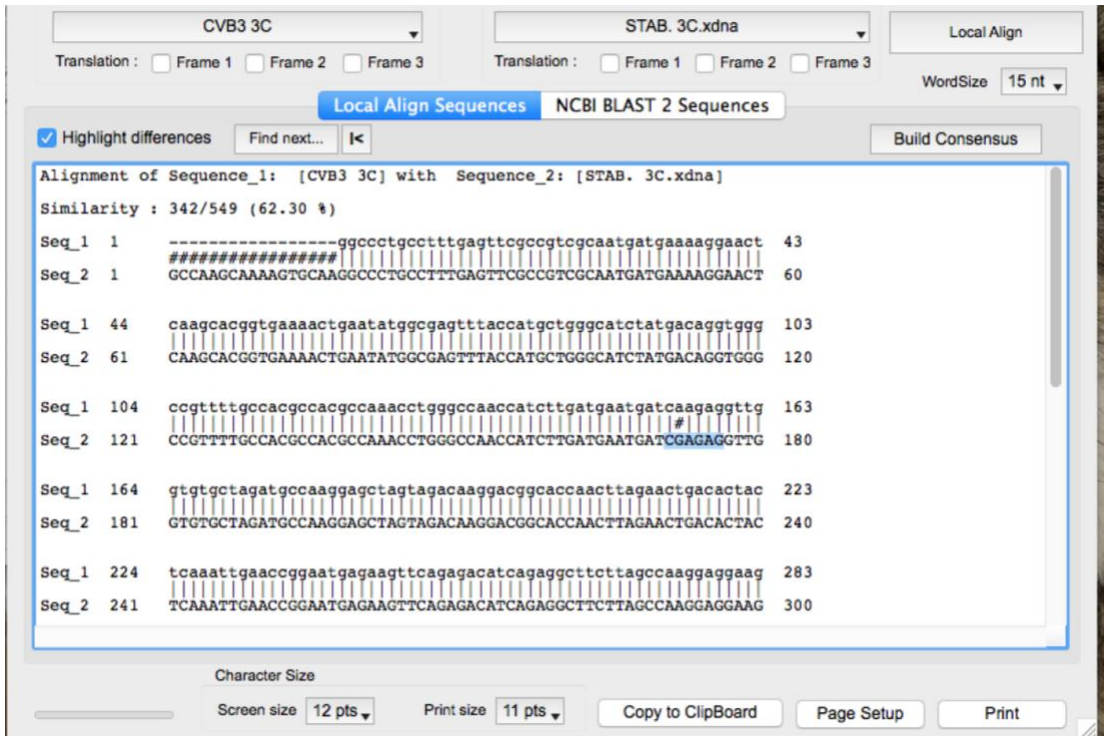

B

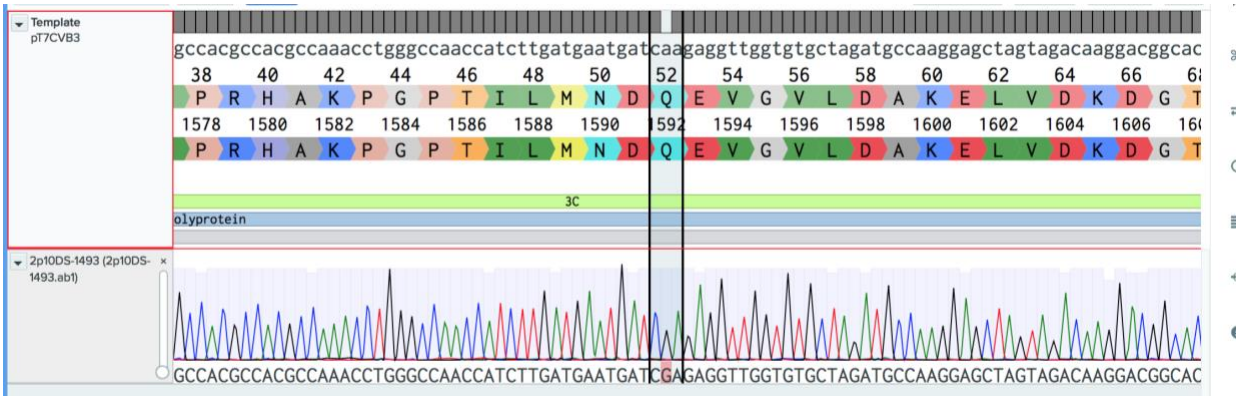

Figure 9. Analysis of the Stability of the 3CQ52R mutant. The $3C^{Q52R}$ mutant was passaged in untreated Vero cells for a total of 5 passages, RNA was then extracted from the supernatant, purified, reverse transcribed than sent off for sequencing. A) Comparative look of the passaged $3C^{Q52R}$ mutant sequence aligned with the WT 3C sequence utilizing serial cloner. Octothorp (#) indicate differences in sequence. Highlighted sequence is the 3C mutation. B) Comparative look of the passaged $3C^{Q52R}$ mutant sequence aligned with the WT sequence utilizing Benchling software. Highlighted portion is the 3C mutation site. Red nucleotides indicate differences from WT sequence.

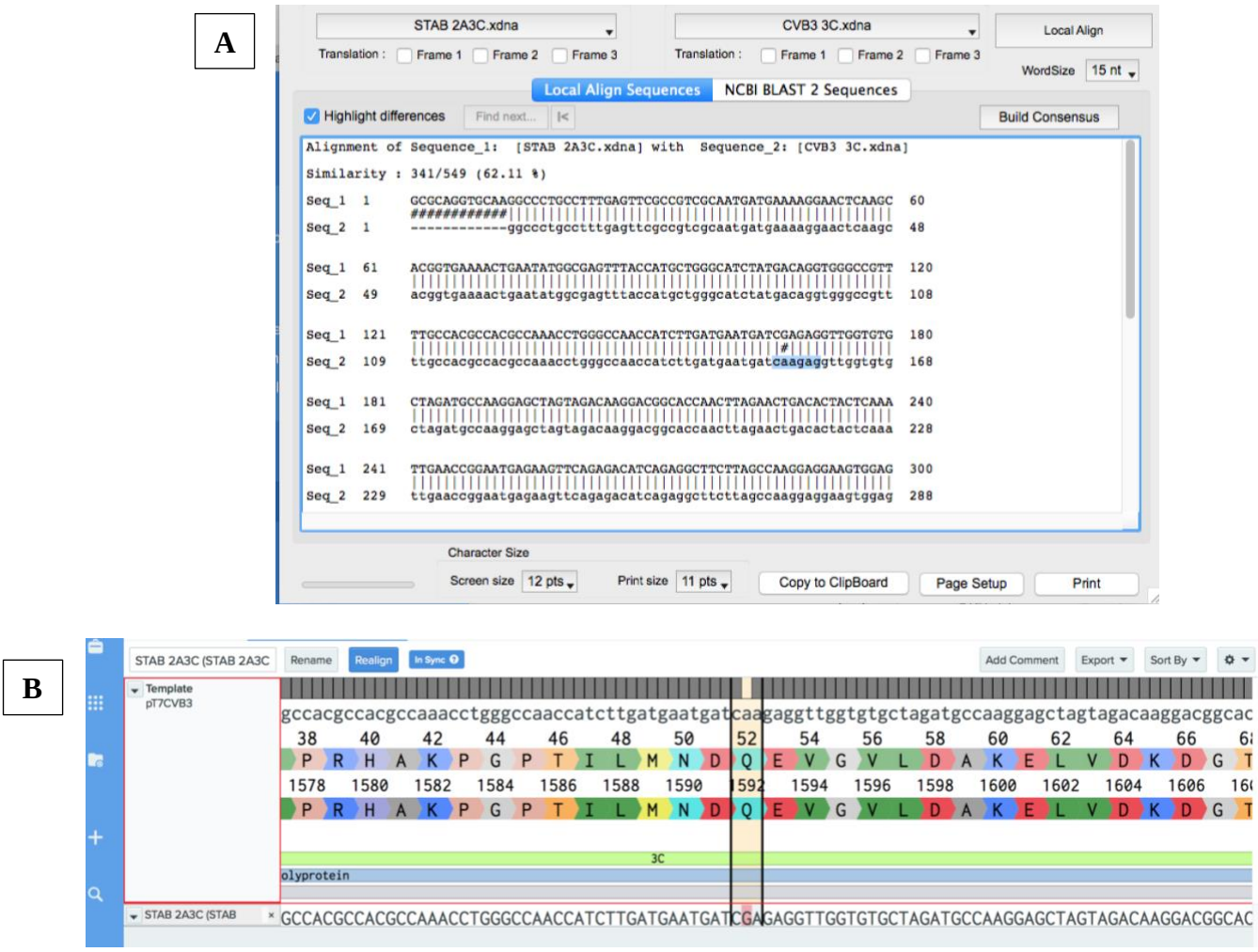

Figure 10. Analysis of the Stability of the 2A^{Q29K} 3C^{Q52R} mutant at the 3C^{Q52R} Mutation Site. The 2A^{Q29K}3C^{Q52R} mutant was passaged in untreated Vero cells for a total of 5 passages, RNA was then extracted from the supernatant, purified, reverse transcribed than sent off for sequencing. The double mutant was sequenced at the 3C mutation site. A) Comparative look of the passaged 2A^{Q29K} 3C^{Q52R} mutant sequence aligned with the WT 3C sequence utilizing serial cloner. Octothorp (#) indicate differences in sequence. Highlighted sequence is the 3C mutation. B) Comparative look of the passaged 2A^{Q29K} 3C^{Q52R} mutant sequence aligned with the WT sequence utilizing Benchling software. Highlighted portion is the 3C mutation site. Red nucleotides indicate differences from WT sequence.

Viral fitness was determined utilizing a similar protocol as the stability assay, with the exception that each virus was mixed with wild-type CVB3 at a 1:1 ratio. This mixture was then used to inoculate Vero cells for 24h and passaged for five rounds. At and at the end of the fifth passage, supernatants were collected, RNA was purified and reverse transcribed, and sent off for

sequencing at the mutation sites (**Figures 11-13)**. Through analyses of the chromatogram, we found that no mutant had a fitness advantage over the WT virus. This is due to the absence of one nucleotide dominating. The presence of a mixed population, two peaks of nucleotides, at the site of the mutation is indicative of no overall fitness advantage. The mixed population shows us that both viruses were present at the 5th passage, meaning neither virus outcompeted the other. It is important to note that this result is strictly qualitative, and is not measure of the abundance of one nucleotide over the other. This result was recapitulated when the plaque sizes of the mutants were compared to wild-type (**Figure 14**).

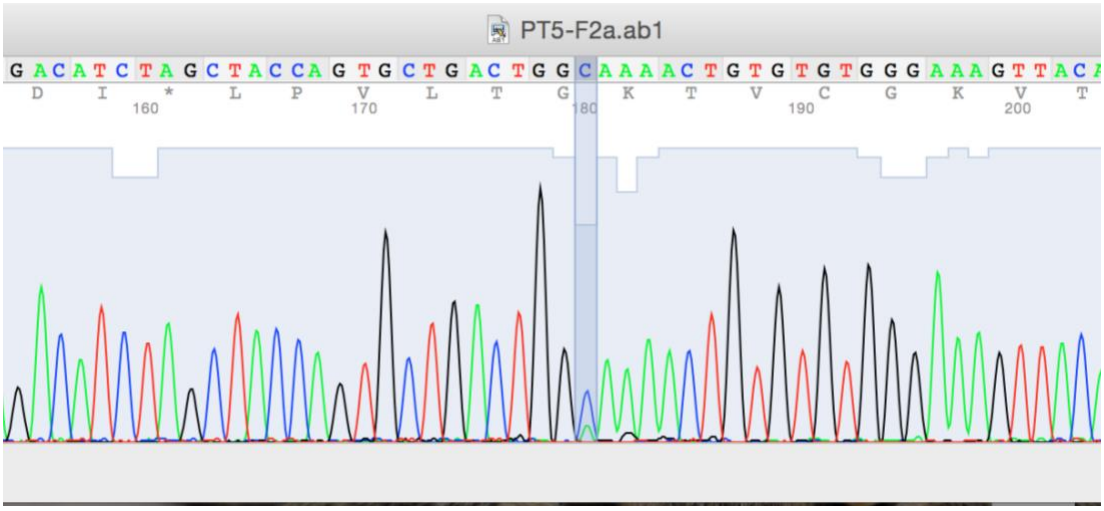

Figure 11. Analysis of the Fitness of the 2A^{Q29K} Mutant Virus vs. WT. Mutant 2A^{Q29K} fitness was measured utilizing a competition assay. Mutant 2A^{Q29K} was mixed with WT CVB3 in a 1:1 ratio, this mixture was used to infect untreated Vero cells and passaged 5 times. The supernatant was then collected, RNA was extracted and purified, reverse transcribed and then sequenced at the 2A mutation site. Results were analyzed via chromatograph. The highlighted portion is the nucleotide site that is mutated in 2A^{Q29K}.

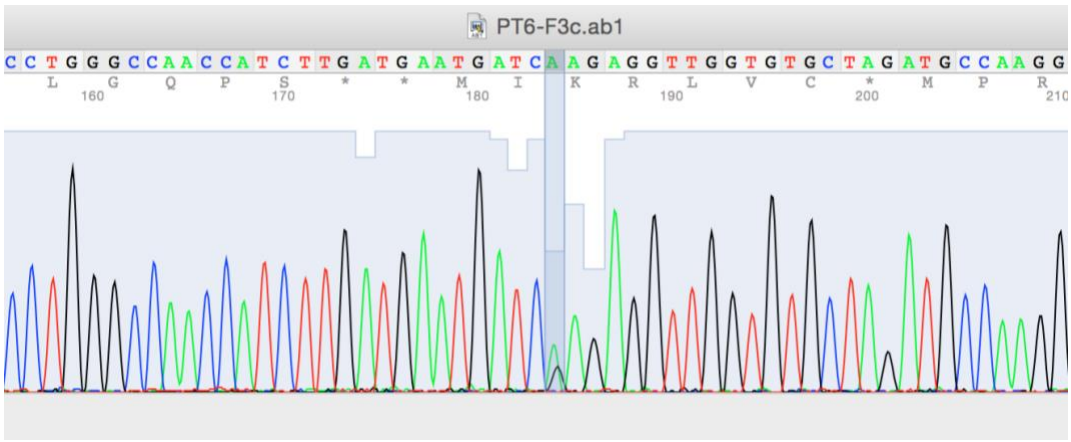

Figure 12. Analysis of the Fitness of the 3C^{Q52R} Mutant Virus vs. WT. Mutant 3C^{Q52R} fitness was measured utilizing a competition assay. Mutant 3C^{Q52R} was mixed with WT CVB3 in a 1:1 ratio, this mixture was used to infect untreated Vero cells and passaged 5 times. The supernatant was then collected, RNA was extracted and purified, reverse transcribed and then sequenced at the 3C mutation site. Results were analyzed via chromatograph. The highlighted portion is the nucleotide site that is mutated in 3C^{Q52R}.

Figure 13. Analysis of the Fitness of the 2A^{Q29K} 3C^{Q52R} Mutant Virus vs. WT. Mutant 2A^{Q29K} 3C^{Q52R} fitness was measured utilizing a competition assay. Mutant 2A^{Q29K} 3C^{Q52R} was mixed with WT CVB3 in a 1:1 ratio, this mixture was used to infect untreated Vero cells and passaged 5 times. The supernatant was then collected, RNA was extracted and purified, reverse transcribed and then sequenced at the 2A mutation site. Results were analyzed via chromatograph. The highlighted portion is the nucleotide site that is mutated in 2A^{Q29K}.

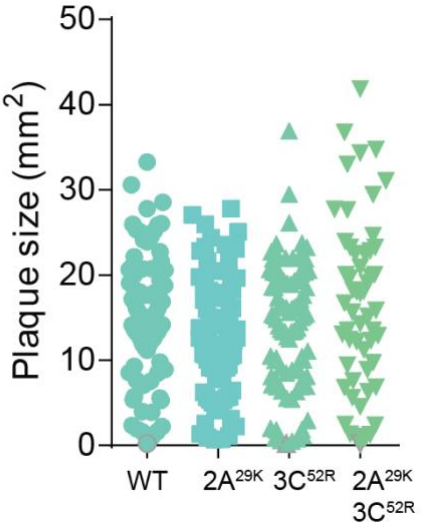

Figure 14. Determination of Viral Fitness via Plaque Assay. Untreated Vero cells were infected with both the WT and mutant viruses at an MOI of 0.1. A plaque assay was then performed to visualize, and the size of the plaques were measured.

Evaluating the Mutants' Resistance to DENSpm

We next wanted to evaluate whether or not these mutations also confer resistance to other polyamine depleting drugs, such as diethylnorspermidine (DENSpm). DENSpm depletes polyamines through accelerating polyamine metabolism by acetylating spermidine and spermine, marking them for export. Vero cells were pretreated with 10µM DENSpm for 16h, or left untreated, the cells were then inoculated with wild-type CVB3, $2A^{Q29K}$, $3C^{Q52R}$, and the $2A^{Q29K}3C^{Q52R}$ mutants at an MOI of 0.1, after 24h the supernatant was collected and titered in order to determine PFU (**Figure 15**). Raw measures of viral titers show a slight rescue of the 2A mutant in the presence of DENSpm but this rescue of viral titer was complete when looking at both the 3C and 2A3C mutant.

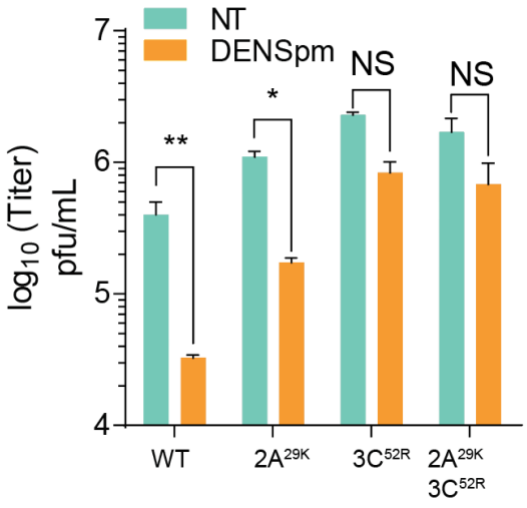

Figure 15. Determining the Sensitivity of the Mutants in DENSpm Compared to NT. Vero cells were treated with 10µM DFMO or left untreated and infected at an MOI of 0.1 with the WT or mutant viruses. At 24 hpi viral titers were enumerated. * $p \leq 0.05$, ** $p \leq 0.01$, *** $p \leq 0.001$ using Student's t-test ($n \geq 3$), comparing treated samples to untreated controls. Error bars represent ± 1 SEM

When looking at the percent replication in DENSpm compared to untreated control all three of the mutants confer partial resistance to DENSpm, most notably the $3C^{Q52R}$ and $2A^{Q29K}3C^{Q52R}$ mutant which both reach about 60% replication in DFMO treated conditions compared to control. This suggests that the mutants were able to replicate 60x better in DFMO than the WT virus (**Figure 16**).

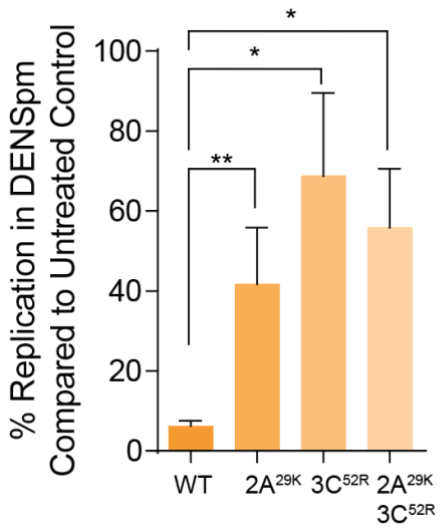

Figure 16. Determining the Percent Replication of the Mutants in DENSpm Conditions Compared to WT. Vero cells were treated with 10µM DFMO and infected at an MOI of 0.1 with the WT or mutant viruses. At 24 hpi viral titers were enumerated. The results are the titers of each respective virus divided by the titer in untreated conditions. * $p \leq 0.05$, ** $p \leq 0.01$, *** $p \leq 0.001$ using Student's t-test ($n \geq 3$), comparing treated samples to untreated controls. Error bars represent ± 1 SEM

Passaging CVB3 in DENSpm

Due to the $2A^{Q29K}$, $3C^{Q52R}$, and the $2A^{Q29K}3C^{Q52R}$ mutants being resistant to DENSpm, we wanted to determine if CVB3 would gain resistance to DENSpm if passaged similarly to the original passages with the exception of utilizing DENSpm rather than DFMO. Vero cells were either pre-treated with 10µM DENSpm or left untreated for 16h and then inoculated with CVB3 at an MOI of 0.1. As mentioned earlier, concentration of DENspm was increased as passaging increased, and each new passage was infected at an MOI of 0.1 to promote bottlenecking. Along with the drug treated condition, untreated cells were also utilized for passaging as a control, as virus passaged in untreated conditions should not gain resistance to polyamine depletion. Supernatant was collected at 24h post-infection, viral titer was determined via plaque assay, and this new titer was then used to infect new Vero cells that had been pretreated with DENSpm at

10µM for 16h with an MOI of 0.1, DENSpm concentration was increased as passaging increased in order to encourage bottlenecking. This process was completed for a total of 10 passages. Through viral titer we observe that the CVB3 that was passaged in the presence of DENSpm had an increase of viral titer(**Figure 17**), suggestive of resistance. **Figure 17** also shows a cyclical pattern, where viral titer drops and then rebounds in the next passage. It is possible that passaging in this way is producing defective virus, where after one passage the only viruses present are viruses that are extremely efficient at replication. The subsequent passage produces viruses that are not as efficient but are still able to infect non-treated cells and produce viable plaques. The next passage that is infected with this non-efficient virus cannot replicate as well in DENSpm treated conditions, therefore only the efficient viruses survive.

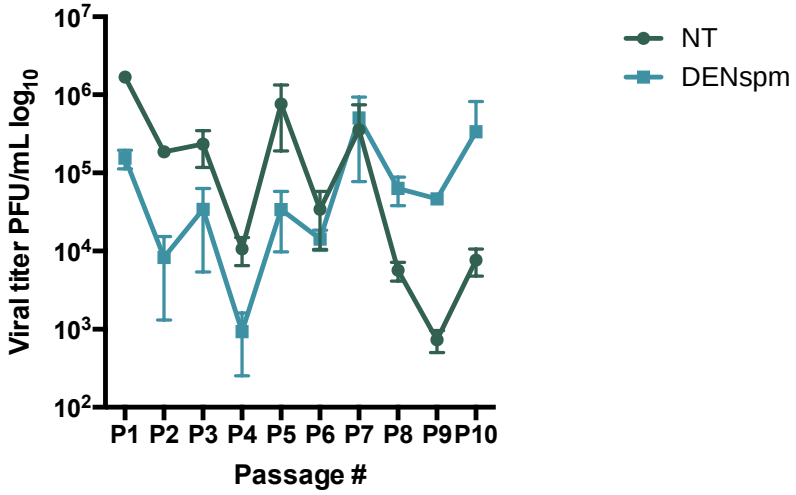

Figure 17. Determining Resistance through Viral Titer. Vero cells were treated with DENSpm and infected with WT CVB3 at an MOI of 0.1, the virus was passaged through fixed passaging and viral titer was determined after each passage. Error bars represent ± 1 SEM

We performed these passages with DENSpm in an uncontrolled manner as well – blind passaging. Vero cells were pretreated with 10µM DENSpm 16h before infection or left untreated, the cells were then infected at an MOI of 0.1. After 24h, 50µL of supernatant was used to inoculate new Vero cells that had previously been pretreated with 20µM DENSpm. This was

done until a total of 10 passages was reached. Increasing in concentrations of DENSpm were used in order to enhance bottlenecking, and the untreated cell passages act as a control. As virus passaged in untreated conditions should not gain resistance to polyamine depletion. At the end of the 10th passage DENSpm sensitivity was investigated. This was done by treating cells with 100µM DENSpm for 16h, inoculating cells with the passaged virus, and 24hpi viral titers were determined via plaque assay. As can be seen in **Figure 18**, after passage 10, the virus gained a partial resistance to DENSpm pretreatment, with untreated virus showing a 19.6x decrease in viral titer and the DENSpm treated virus having a 7x decrease in viral titer, compared to non-treated conditions. This suggested the development of limited resistance in the DENSpm passaged virus.

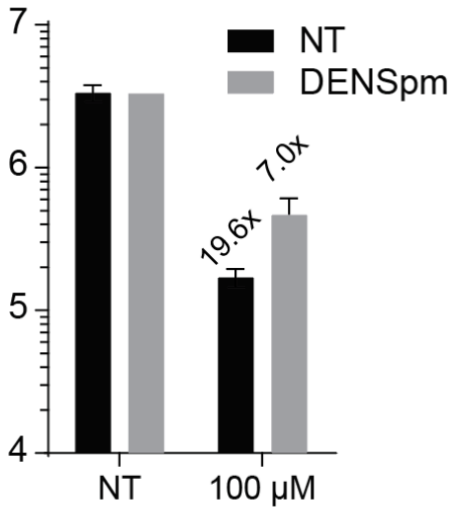

Figure 18. Determining Passaged Virus Sensitivity to DENSpm. Vero cells were treated with DENSpm and infected with WT CVB3 at an MOI of 0.1, the virus was passaged through blind passaging. After the 10th passage virus was collected and tested for its sensitivity to DENSpm. Vero cells were treated for 16hs with 100µM DENSpm and infected with the blind passaged virus. Error bars represent ± 1 SEM

CVB3 Protease activity being Modulated by Polyamines

Due to the 2A^{Q29K}, 3C^{Q52R}, and the 2A^{Q29K}3C^{Q52R} mutants developing resistance to polyamine depletion, we hypothesized that polyamines modulate protease activity. To directly measure

proteolytic activity with or without polyamines we generated a protease-sensitive dual luciferase reporter system. A schematic of which can be seen in **Figure 19**. In this luciferase system, cleavage of a target sequence allows for firefly luciferase activity, which was normalized to a Renilla luciferase transfection control. This system has previously been established to examine viral proteases, but this has not been extended to CVB3 2A or 3C proteases [68–70]. In order to generate this system, we cloned a 2A target sequence -MTNTGAFG - and a 3C target sequence – SAMEQG- into the firefly luciferase reporter [71]. We also cloned the 2A and 3C CVB3 proteases into the pCMV plasmid to drive robust protease expression. These constructs were co-transfected into 293T cells that had either been pre-treated with increasing concentrations of DFMO for 4days or left untreated. Firefly activity was measured as luminescence at 24h hpi and normalized to Renilla activity (**Figure 20**). The data shows that with increasing concentrations of DFMO the proteolytic activity significantly decreases, indicative of viral proteases being reliant upon polyamines for functionality.

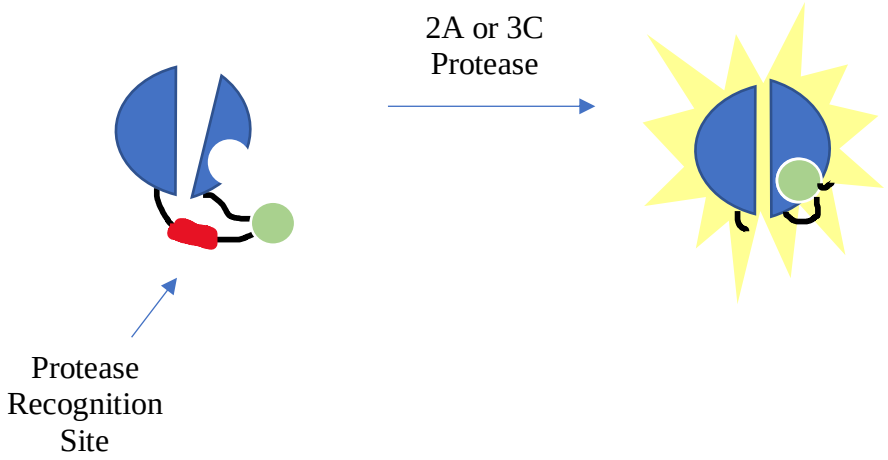

Figure 19. Depiction of the Protease Assay which Utilizes Luciferase Activity. The target substrate contains a protease recognition site, once recognized, the 2A or 3C protease cleaves said site and the substrate confers a conformational change which allows for robust luciferase activity.

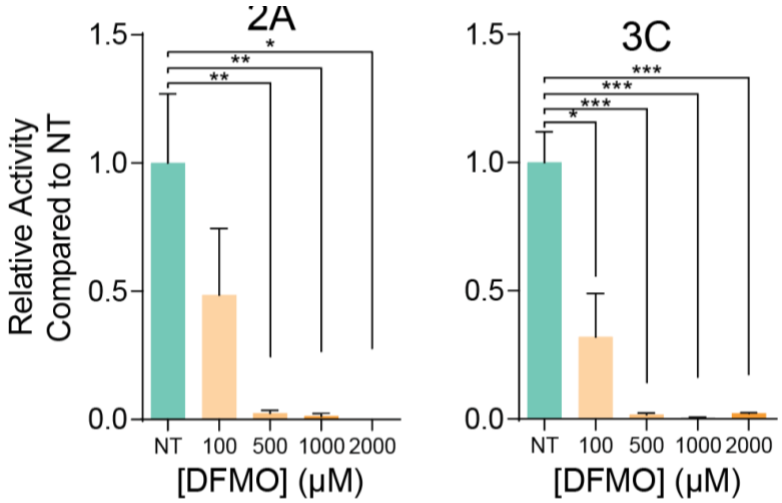

Figure 20. Determining the Viral Proteases Sensitivity to DFMO Treatment. Utilizing the protease assay, viral protease activity was testing in a variety of DFMO concentrations. The results were normalized first to Renilla activity then to NT conditions.* $p \leq 0.05$, ** $p \leq 0.01$, *** $p \leq 0.001$ using Student's t-test ($n \geq 3$), comparing treated samples to untreated controls. Error bars represent ± 1 SEM

In order to look at the protease activity *in vitro*, specifically the cellular targets of 2A and 3C, we treated cells with increasing doses of DFMO and DENSpm to deplete cellular polyamines. Following incubation with drug, cells were infected at an MOI of 10 for 24h, and cellular lysates were then collected for western analysis. Higher MOI was utilized in order to get robust cleavge of the cellular target. Lysates were analyzed for the presence of cleaved eIF4G, a cellular target for the viral proteases (**Figure 21**). The data displayed shows that in infected cells, a distinct eIF4G band was present; however, in cells treated with either DFMO or DENSpm, the eIF4G cleavage is significantly inhibited.

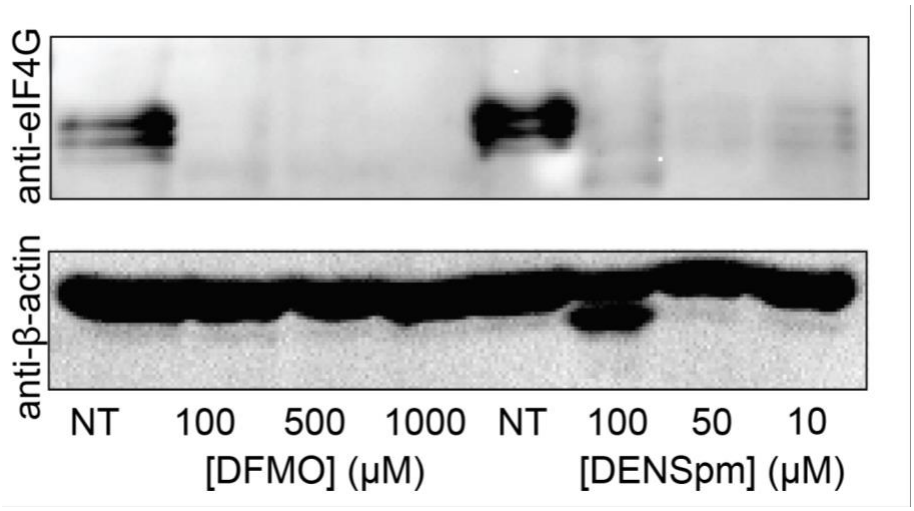

Figure 21. Determining the Virus's ability to Cleave Cellular Targets in Polyamine Depleting Drugs. Viral cellular target, eIF4G, cleavage was monitored in virally infected cells in the presence or absence of both DFMO and DENSpm.

CVB3 Mutant Protease activity being resistant to polyamine depletion

Due to mutations occurring in these protease regions, we hypothesized that these mutations may be able to maintain viral protease activity even in the absence of polyamines. In order to test this, we generated mutant $2A^{Q29K}$ and $3C^{Q52R}$ proteases through site-directed mutagenesis of our overexpression vectors. We then co-transfected these proteases and wild-type controls with our luciferase reporter system into 293T cells that had either been treated with 500μM DFMO for 4days or left untreated. After 24h, we measured luciferase activity as luminescence and normalized to Renilla luciferase activity and to control cells transfected with the luciferase reporter alone (no protease) (**Figure 22**). It was observed that both the wild-type 2A protease as well as the 3C wild-type protease exhibited decreased protease activity in the presence of DFMO. However, both the $2A^{Q29K}$ and $3C^{Q52R}$ mutant had robust protease activity in both the nontreated and DFMO treated conditions. It can also be seen that the mutant 3C protease has higher proteolytic activity than the wild-type but this same phenomenon is not seen in the 2A protease.

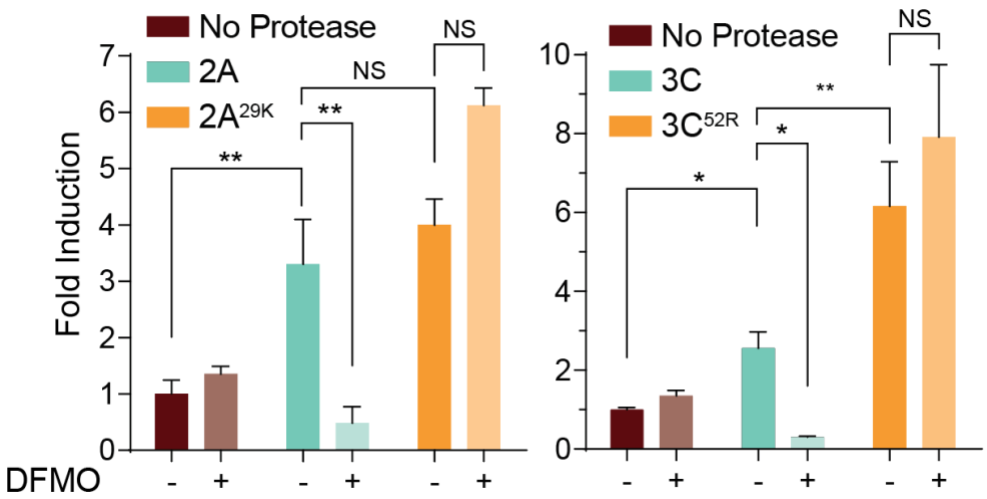

Figure 22. Determining the Viral Mutants Ability to Resist DFMO Treatment. Wildtype and Mutant CVB3 protease activity was monitored via the protease assay in either untreated or polyamine depleted conditions. The results were normalized, first to the renilla control, then to the no protease conditions.* $p \leq 0.05$, ** $p \leq 0.01$, *** $p \leq 0.001$ using Student's t-test ($n \geq 3$), comparing treated samples to untreated controls. Error bars represent ± 1 SEM

We further hypothesized that mutant protease activity may enhance proteolytic cleavage of a cellular target during viral infection to enhance virus replication. To investigate this, we treated Vero cells with 500µM DFMO for 4d or left cells untreated and then infected at an MOI of 10 for 24h. Cell lysates were collected and analyzed for cleavage of eIF4G (**Figure 23)**. In untreated cells, we observed significant cleavage of eIF4G with WT infection and similar levels of cleavage with infection of the $2A^{Q29K}$, $3C^{Q52R}$, and the $2A^{Q29K}3C^{Q52R}$ mutants. However, with DFMO treatment, eIF4G was significantly reduced in WT CVB3 virus as was previously observed, but proteolytic cleavage in the mutant viruses was significantly higher than that of WT.

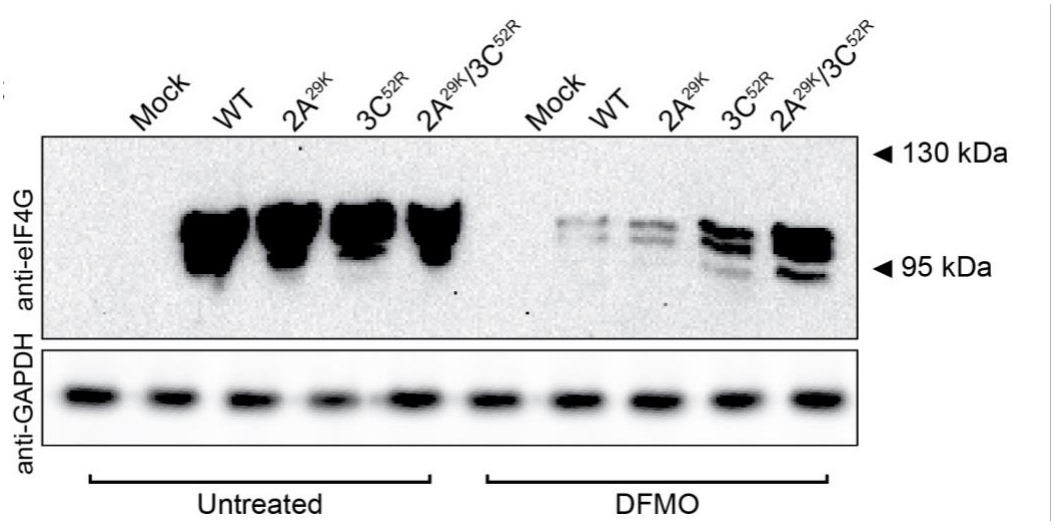

Figure 23. Elucidating the Mutant Virus's ability to Cleave Cellular Targets (eIF4G) in the Presence of DFMO. The ability of the mutant and wildtype viruses ability to cleave eIF4G in the presence of DFMO was monitored via western blot.

A similar experiment was done using DENSpm as the polyamine depleting drug (**Figure S4**). We observed cleavage of eIF4G was only partially rescued in mutant viruses. Nonetheless, the cleavage was less pronounced than in the DFMO treated conditions. This further suggests that DENSpm might disrupt the cell differently than DFMO, given that DENSpm leaves putrescene in the cell due to its mechanism of action, which can be seen in **Figure 2.**

CHAPTER FOUR: DISCUSSION

Escape Mutants

Viral escape mutants are an important tool in studying multiple facets of RNA virus replication [72]. Here, our utilization of drug treatment to produce these viral escape mutants provides a better understanding as to how the virus is able to mutate in order to resist antiviral treatment, which, in turn, allows us to understand mechanisms as to how the antiviral is actually affecting the virus. In the case of drugs such as DFMO and DENSpm, escape mutants offer a better understanding not only of how these drugs are affecting the virus, but also how polyamines, specifically, are interacting with RNA viruses. It also provides insight as to what stage in the viral lifecycle polyamines are having a direct role. Subsequently, passaging gives us an understanding as to what mutations are necessary for CVB3 to gain resistance to polyamine depletion. Previously, chikungunya virus escape mutants from DFMO treatment, were characterized and found to confer resistance when simultaneously present in the virus [48]. Unlike, CHIKV, we found that CVB3 gains resistance to DFMO treatment from a single mutation in either protease. Although we cannot determine whether polyamines help viral protease activity against a specific target, we observe that these mutations help viral infection in an otherwise antiviral environment. Determining the specifics of this interaction is an important area of study.

Characterization of Escape Mutants

Passaging CVB3 in the presence of DFMO resulted in two mutations, both of which involved changing from a neutral glutamine residue to a positively charged lysine or arginine. Interestingly, we observed similar amino acid changes from our CHIKV passages [48], where a glycine to arginine mutation was observed in the nsP1 region of the viral genome. Polyamines are positively charged molecules at a physiological pH, therefore, the appearance of positively-charged amino acids due to polyamine depleted conditions suggests that these mutations are due to viral compensation from losing polyamines in the environment. The mutations we observe in the 2A and 3C protease region of CVB3 are not in the active site of either enzyme [65,73]. This suggests that these amino acids, with their positive charge, are affecting the active site of these enzymes allosterically. How exactly this is occurring remains unknown.

Importantly, as was alluded to previously, these single mutations in the protease confer resistance to both DFMO and DENSpm treatment. There is a significant rescue of viral titer, which can be seen in our sensitivity assays. These data suggest that this single amino acid change, to a positively charged residue is enough to partially rescue viral infectivity.

When comparing the fitness of mutant viruses to WT we saw no fitness advantage of one over the other, contrary to what was seen in CHIKV mutants [48]. The specific infectivity of the mutations was not affected either, as can be seen in **Supplemental Figures 3 A, B and C**. However, these mutations can withstand polyamine-depleted conditions. This result suggests that even if the virus were to emerge, the mutation may not fix a population if not exposed to DFMO.

DENSpm Escape Mutants

We also looked at viral escape mutants utilizing DENSpm as the polyamine depleting vehicle rather than DFMO. After 10 passages, both through controlled, fixed MOI passaging,

and blind passaging, viruses that survived exhibited a partial resistance to DENSpm treatment. Further testing will need to be done in order to determine the mutation(s) that arose as well as whether this also conferred resistance to DFMO treatment.

Polyamines and Viral Protease Activity

The placement of the mutations as well as our data suggests a novel function of polyamines in protease activity. Although it has been observed that polyamines contribute to protease activity [74] of plant and eukaryotic proteases, a function for polyamines in viral protease activity has not been described. Specifically, spermidine interacts with and activates the activity of mammalian chymotrypsin[75]. The broader implications of polyamines and protease activity, especially related to viral protease activity, have not been explored beyond this study. Our data supports the idea that polyamines contribute to the function of viral proteases [76].

In general, targeting polyamines synthesis as a therapeutic method offers great potential as the availability of FDA-approved molecules like DFMO allows for the potential of inhibition of this pathway that is key for successful viral infection. Again, the appearance of these resistance mutation from single amino acid changes necessitate combination therapy in order to combat this resistance emerging, especially considering the fitness of these mutant viruses are not greater than that of WT in non-DFMO treated conditions.

Overall these data suggest that these mutations are not enhancing protease activity, at least in the case of 2A, and therefore must be extremely specific to polyamines. Interestingly, it seems that DFMO and DENSpm, although both polyamine depleting drugs, might disturb viral replication in different ways, as illustrated by **Supplemental Figure 4**. The putrescene that is left in the system from DENSpm treatment, due to the mechanism of action of DENSpm as shown in **Figure 2,** might have some effect on these mutants and their ability to infect cells. With this in

mind, examining and characterizing the viral escape mutants from the DENSpm passages will be an interesting area to study and follow-up on in order to determine this complex relationship.

Overall this thesis offers insight and new evidence as to how polyamines contribute to viral protease activity and suggests a potential target for antiviral therapy to combat CVB3 and potentially other viruses.

APPENDIX: SUPPLEMENTAL FIGURES

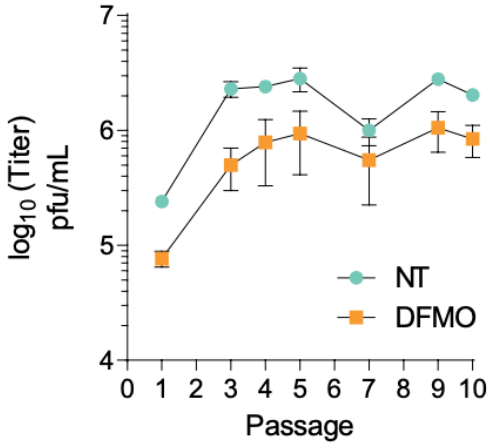

Figure S1. CVB3 Develops Resistance to Polyamine Depletion Over Passages with Polyamine-Depleting Molecules. Vero-E6 cells were left untreated of treated with 500μM DFMO for four days prior to infection with CVB3 at an MOI of 0.1. Virus was collected at 24hpi and used to infect the next passage. Viral Titers were determined via plaque assay. Error bars represent ± 1 SEM

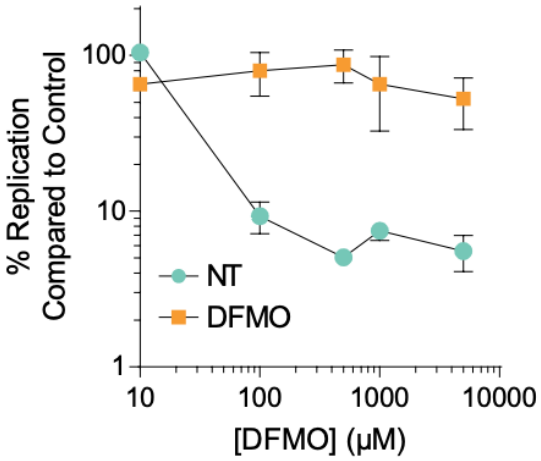

Figure S2. After Passage Five CVB3 Shows Resistance to Polyamine Depletion. CVB3 passaged five times over Vero-E6 cells, either treated with 500 μM DFMO or untreated, were used to infect Vero cells treated with increasing doses of DFMO for 24 hpi. Viral Titers were determined via plaque assay. Error bars represent ± 1 SEM

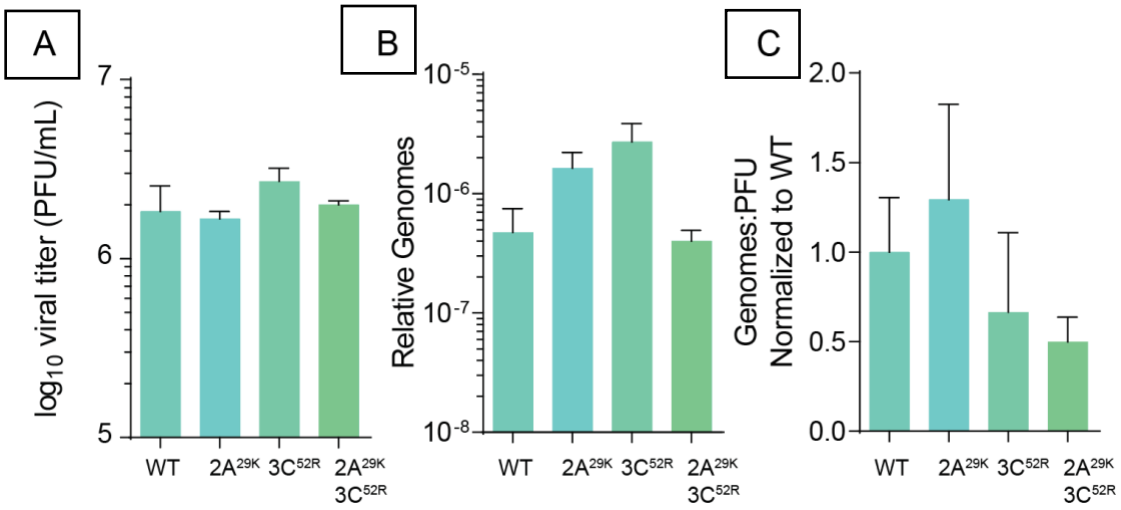

Figure S3. Specific Infectivity is not Altered with Protease Mutation. Vero cells were infected with WT and mutant CVB3 for 24hr at which time viral titers were determined by plaque assay (A) and viral genomes in cell supernatant were determined via qPCR (B). The ratio of genomes-to-PFU (C) was calculated by dividing he relative genomes in (B) by the titer in (A). Error bars represent ± 1 SEM

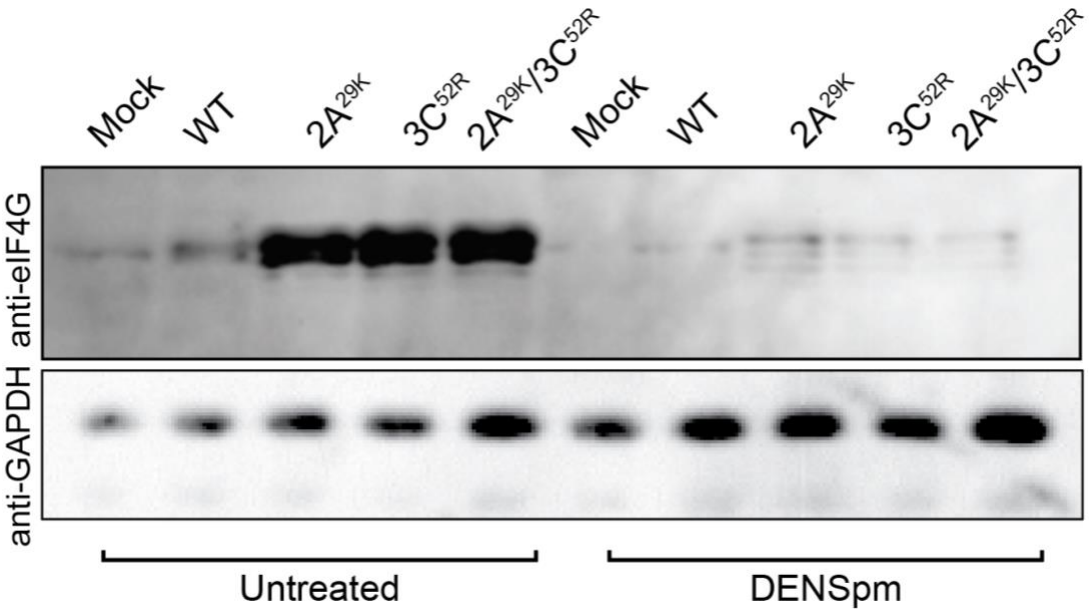

Figure S4. Assessing the Mutant Virus's ability to Cleave Cellular Targets (eIF4G) in the Presense of DENSpm. The ability of the mutant and WT viruses ability to cleave eIF4G in the presense of DENSpm, another polyamine depleting drug, was monitored via western blot.

REFERENCE LIST

1. van der Linden L, Wolthers KC, van Kuppeveld FJM. Replication and inhibitors of enteroviruses and parechoviruses. *Viruses*. 2015;7(8):4529-4562. doi:10.3390/v7082832

2. Marchant D, Hendry R, Yang D, et al. Coxsackievirus B3 replication and pathogenesis. *Future Microbiol*. 2015;10(4):629-653. doi:10.2217/fmb.15.5

3. Dan M, Chantler JK. A Genetically Engineered Attenuated Coxsackievirus B3 Strain Protects Mice against Lethal Infection. *J Virol*. 2005;79(14):9285-9295. doi:10.1128/jvi.79.14.9285-9295.2005

4. Olsen K. Clear Waters and a green gas: A history of chlorine as a swimming pool sanitizer in the united states. *Bull Hist Chem*. 2007;32(2):129-140. http://acshist.scs.illinois.edu/bulletin_open_access/v32-2/v32-2 p129-140.pdf.

5. McGeady ML, Siak JS, Crowell RL. Survival of coxsackievirus B3 under diverse environmental conditions. *Appl Environ Microbiol*. 1979;37(5):972-977.

6. O'Brien RT, Newman JS. Inactivation of polioviruses and coxsackieviruses in surface water. *Appl Environ Microbiol*. 1977;33(2):334-340.

7. Tian L, Yang Y, Li C, et al. The cytotoxicity of coxsackievirus B3 is associated with a blockage of autophagic flux mediated by reduced syntaxin 17 expression article. *Cell Death Dis*. 2018;9(2). doi:10.1038/s41419-018-0271-0

8. Lee CJ, Huang YC, Yang S, et al. Clinical features of coxsackievirus A4, B3 and B4 infections in children. *PLoS One*. 2014;9(2). doi:10.1371/journal.pone.0087391

9. Matteucci D, Paglianti M, Giangregorio AM, Capobianchi MR, Dianzani F, Bendinelli M. Group B Coxsackieviruses Readily Establish Persistent Infections in Human Lymphoid Cell Lines. *J Virol*. 1985;56(2):651-654.

10. Benz HL. Update on Coxsackievirus B3 Myocarditis. *HHS Public Access*. 2017;24(4):1-10. doi:10.1109/EMBC.2016.7590696.Upper

11. Yajima T. Viral myocarditis: potential defense mechanisms within the cardiomyocyte against virus infection. *NIH Public Access*. 2012;29(6):997-1003. doi:10.1016/j.biotechadv.2011.08.021.Secreted

12. Howlett SE. Coxsackievirus B3-Induced Myocarditis: New Insights Into a Female Advantage. *Can J Cardiol*. 2018;34(4):354-355. doi:10.1016/j.cjca.2018.01.086

13. Lal A, Akhtar J, Isaac S, et al. Unusual cause of chest pain, Bornholm disease, a forgotten entity; case report and review of literature. *Respir Med Case Reports*. 2018;25(October):270-273. doi:10.1016/j.rmcr.2018.10.005

14. Dennert R, Crijns HJ, Heymans S. Acute viral myocarditis. 2008:2073-2082. doi:10.1093/eurheartj/ehn296

15. Schultz JC, Hilliard AA, Jr LTC, Rihal CS. Diagnosis and Treatment of Viral Myocarditis. 2009;84(November):1001-1009.

16. Sellier P, Lopes A, Morgand M, et al. Etiologies and Management of Aseptic Meningitis in Patients Admitted to an Internal Medicine Department. 2016;95(2):1-9. doi:10.1097/MD.0000000000000237

17. Mounce BC, Olsen ME, Vignuzzi M, Connor JH. Polyamines and Their Role in Virus Infection. *Microbiol Mol Biol Rev*. 2017;81(4):e00029-17. doi:10.1128/MMBR.00029-17

18. Pegg AE. Functions of Polyamines in Mammals*. *Minireview*. 2016;291(29):14904-14912. doi:10.1074/jbc.R116.731661

19. Hogarty MD, Norris MD, Davis K, et al. ODC1 is a critical determinant of MYCN oncogenesis and a therapeutic target in neuroblastoma. *NIH Public Access*. 2009;68(23):9735-9745. doi:10.1158/0008-5472.CAN-07-6866.ODC1

20. Brooks WH. Increased polyamines alter chromatin and stabilize autoantigens in autoimmune diseases. *Front Immunol*. 2013;4(APR):1-8. doi:10.3389/fimmu.2013.00091

21. Childs AC, Mehta DJ, Gerner EW. Cellular and Molecular Life Sciences Polyamine-dependent gene expression. 2003;60:1394-1406. doi:10.1007/s00018-003-2332-4

22. Gerner EW, Meyskens FL. Polyamines and cancer: Old molecules, new understanding. *Nat Rev Cancer*. 2004;4(10):781-792. doi:10.1038/nrc1454

23. Frugier M, Florentz C, Hosseini MW, Lehn J marie, Giegé R. Synthetic polyamines stimulate in vitro transcription by T7 RNA polymerase. *Nucleic Acids Res*. 1994;22(14):2784-2790. doi:10.1093/nar/22.14.2784

24. Mandal S, Mandal A, Johansson HE, Orjalo A V., Park MH. Depletion of cellular polyamines, spermidine and spermine, causes a total arrest in translation and growth in mammalian cells. *Proc Natl Acad Sci*. 2013;110(6):2169-2174. doi:10.1073/pnas.1219002110

25. Manuscript A. Genome packaging in viruses. 2011;20(1):114-120.

doi:10.1016/j.sbi.2009.12.006.Genome

26. Gibson W. Compartmentalization of Spermine and Spermidine in the Herpes Simplex Virion. 1971;68(11):2818-2821.

27. Lanzer W, Holowczak JA. Polyamines in Vaccinia Virions and Polypeptides Released from Viral Cores by Acid Extraction. 1975;16(5):1254-1264.

28. Britain G. The Effect of Polyamines on Herpes Simplex Virus Type 1 D N A Polymerase Purified from Infected Baby Hamster Kidney Cells (BHK-21/C13). 2019;(May):397-400.

29. Wallace HM, Baybutt HN, Pearson CK, Keir HM. Effect of Spermine on the Activity of Herpes Simplex Virus Type 1 DNA Polymerase. *FEBS Lett*. 1981;126(2).

30. Kenyon TK, Lynch J, Hay J, Ruyechan W. Varicella-Zoster Virus ORF47 Protein Serine Kinase : Characterization of a Cloned , Biologically Active Phosphotransferase and Two Viral Substrates , ORF62 and ORF63. 2001;75(18):8854-8858. doi:10.1128/JVI.75.18.8854

31. Mounce BC, Poirier EZ, Passoni G, et al. Interferon-Induced Spermidine-Spermine Acetyltransferase and Polyamine Depletion Restrict Zika and Chikungunya Viruses. *Cell Host Microbe*. 2016;20(2):167-177. doi:10.1016/j.chom.2016.06.011

32. Mounce BC, Cesaro T, Moratorio G, et al. Inhibition of Polyamine Biosynthesis Is a Broad-Spectrum Strategy against RNA Viruses. *J Virol*. 2016;90(21):9683-9692. doi:10.1128/JVI.01347-16

33. Tuomi K, Rainat A, Mantyjarvi R. Synthesis of Semliki-Forest virus in polyamine-depleted baby-hamster kidney cells. 1982:113-119.

34. December FL, Raina A. INHIBITION OF SEMLIKI FOREST AND HERPES SIMPLEX VIRUS PRODUCTION IN (II-DIFLUOROMETHYLORNITHINE-TREATED CELLS: REVERSAL BY POLYAMINES K. TUOMI, R. MANTYJARVI and A. RAINA*. 1980;121(2):292-294.

35. Olsen ME, Filone M, Rozelle D, et al. Polyamines and Hypusination Are Required for Ebolavirus Gene Expression and Replication. 2016;7(4):1-10. doi:10.1128/mBio.00882-16.Invited

36. Bevec D, Jaksche H, Oft M, et al. Inhibition of HIV-1 Replication in Lymphocytes by Mutants of the Rev Cofactor eIF-5A. 1996;271(March):1858-1861.

37. Sam CC, Liu J, Henao-mejia J, Liu H. Translational Regulation of HIV-1 Replication by HIV-1 Rev. 2011:308-321. doi:10.1007/s11481-011-9265-8

38. Hoque M, Hanauske-abel HM, Palumbo P, et al. Inhibition of HIV-1 gene expression by

Ciclopirox and Deferiprone , drugs that prevent hypusination of eukaryotic initiation factor 5A. 2009;17. doi:10.1186/1742-4690-6-90

39. Gerner EW, Bruckheimer E, Cohen A. Cancer pharmacoprevention: Targeting polyamine metabolism to manage risk factors for colon cancer. *J Biol Chem*. 2018;293(48):18770-18778. doi:10.1074/jbc.TM118.003343

40. C.J. F, B.F. K, D.A. B, et al. A phase II breast cancer chemoprevention trial of oral (alpha)-difluoromethylornithine: Breast tissue, imaging, and serum and urine biomarkers. *Clin Cancer Res*. 2002;8(10):3105-3117. http://www.embase.com/search/results?subaction=viewrecord&from=export&id=L35155020%5Cnhttp://sfx.library.uu.nl/utrecht?sid=EMBASE&issn=10780432&id=doi:&atitle=A+phase+II+breast+cancer+chemoprevention+trial+of+oral+α-difluoromethylornithine%3A+Breast+tis.

41. Diab DL, Yerian L, Schauer P, et al. The Effect of Difluoromethylornithine on Decreasing Prostate Size and Polyamines in Men: Results of a Year-Long Phase IIb Randomized Placebo-Controlled Chemoprevention Trial. *NIH Public Access*. 2009;6(11):1249-1254. doi:10.1016/j.cgh.2008.07.016.Cytokeratin

42. Vanrell MC, Cueto JA, Barclay JJ, et al. Polyamine depletion inhibits the autophagic response modulating Trypanosoma cruzi infectivity. *Autophagy*. 2013;9(7):1080-1093. doi:10.4161/auto.24709

43. Huaman MA, Fiske CT, Jones TF, et al. Viral Evolution and Epidemiology. *HHS Public Access*. 2015;143(5):951-959. doi:10.1017/S0950268814002131.Tuberculosis

44. Ali SM, Amroun A, Lamballerie X De, Nougairède A. Evolution of Chikungunya virus in mosquito cells. 2018;(July 2017):1-12. doi:10.1038/s41598-018-34561-x

45. Ciota AT, Lovelace AO, Ngo KA, et al. Cell-specific adaptation of two flaviviruses following serial passage in mosquito cell culture. *NIH Public Access*. 2012;357(2):165-174. doi:10.1016/j.virol.2006.08.005.Cell-specific

46. Moser LA, Boylan BT, Moreira FR, et al. Growth and adaptation of Zika virus in mammalian and mosquito cells. 2018:1-19. doi:10.1371/journal.pntd.0006880

47. Perez-Cidoncha M, Killip MJ, Oliveros JC, et al. An Unbiased Genetic Screen Reveals the Polygenic Nature of the Influenza Virus Anti-Interferon Response. *J Virol*. 2014;88(9):4632-4646. doi:10.1128/JVI.00014-14

48. Mounce BC, Cesaro T, Vlajnić L, et al. Chikungunya Virus Overcomes Polyamine Depletion by Mutation of nsP1 and the Opal Stop Codon To Confer Enhanced Replication and Fitness. *J Virol*. 2017;91(15):e00344-17. doi:10.1128/JVI.00344-17

49. Sangar D V. The Replication of Picornaviruses. *J gen Virol*. 1979;45:1-13.

50. Nieva JL, Madan V, Carrasco L. Viroporins: Structure and biological functions. *Nat Rev Microbiol*. 2012;10(8):563-574. doi:10.1038/nrmicro2820

51. Feng Q, Langereis MA, Lork M, et al. Enterovirus 2Apro Targets MDA5 and MAVS in Infected Cells. *J Virol*. 2014;88(6):3369-3378. doi:10.1128/jvi.02712-13

52. Belsham GJ, McInerney GM, Ross-Smith N. Foot-and-mouth disease virus 3C protease induces cleavage of translation initiation factors eIF4A and eIF4G within infected cells. *J Virol*. 2000;74(1):272-280. doi:10.1128/JVI.74.1.272-280.2000

53. W. G, T. S. Extremely efficient cleavage of eIF4G by picornaviral proteinases L and 2A in vitro. *FEBS Lett*. 2000;480(2-3):151-155. doi:10.1016/S0014-5793(00)01928-1

54. Hanson PJ, Ye X, Qiu Y, et al. Cleavage of DAP5 by coxsackievirus B3 2A protease facilitates viral replication and enhances apoptosis by altering translation of IRES-containing genes. *Cell Death Differ*. 2016;23(5):828-840. doi:10.1038/cdd.2015.145

55. Qiu Y, Ye X, Zhang HM, et al. Cleavage of osmosensitive transcriptional factor NFAT5 by Coxsackieviral protease 2A promotes viral replication. *PLoS Pathog*. 2017;13(12):1-28. doi:10.1371/journal.ppat.1006744

56. Xie L, Lu B, Zheng Z, et al. The 3C protease of enterovirus A71 counteracts the activity of host zinc-finger antiviral protein (ZAP). *J Gen Virol*. 2018;99(1):73-85. doi:10.1099/jgv.0.000982

57. Chen K-R, Yu C-K, Kung S-H, et al. Toll-Like Receptor 3 Is Involved in Detection of Enterovirus A71 Infection and Targeted by Viral 2A Protease. *Viruses*. 2018;10(12):689. doi:10.3390/v10120689

58. Wu S, Wang Y, Lin L, et al. Protease 2A induces stress granule formation during coxsackievirus B3 and enterovirus 71 infections. *Virol J*. 2014;11(1):1-10. doi:10.1186/s12985-014-0192-1

59. Visser LJ, Langereis MA, Rabouw HH, et al. Essential role of enterovirus 2A protease in counteracting stress granule formation and the induction of type I interferon. *J Virol*. 2019;(March). doi:10.1128/jvi.00222-19

60. Marcotte LL, Wass AB, Gohara DW, et al. Crystal Structure of Poliovirus 3CD Protein: Virally Encoded Protease and Precursor to the RNA-Dependent RNA Polymerase. *J Virol*. 2007;81(7):3583-3596. doi:10.1128/jvi.02306-06

61. Kim BK, Cho JH, Jeong P, et al. Benserazide, the first allosteric inhibitor of Coxsackievirus B3 3C protease. *FEBS Lett*. 2015;589(15):1795-1801. doi:10.1016/j.febslet.2015.05.027

62. Lim BK, Yun SH, Ju ES, et al. Soluble Coxsackievirus B3 3C Protease Inhibitor Prevents Cardiomyopathy in an Experimental Chronic Myocarditis Murine Model. *Virus Res*. 2015;199:1-8. doi:10.1016/j.virusres.2014.11.030

63. Kim B-K, Ko H, Jeon E-S, Ju E-S, Jeong LS, Kim Y-C. 2,3,4-Trihydroxybenzyl-hydrazide analogues as novel potent coxsackievirus B3 3C protease inhibitors. *Eur J Med Chem*. 2016;120:202-216. doi:10.1016/j.ejmech.2016.03.085

64. Byrd MP, Zamora M, Lloyd RE. Translation of eukaryotic translation initiation factor 4GI (eIF4GI) proceeds from multiple mRNAs containing a novel cap-dependent internal ribosome entry site (IRES) that is active during poliovirus infection. *J Biol Chem*. 2005;280(19):18610-18622. doi:10.1074/jbc.M414014200

65. Cai Q, Yameen M, Liu W, et al. Conformational Plasticity of the 2A Proteinase from Enterovirus 71. *J Virol*. 2013;87(13):7348-7356. doi:10.1128/jvi.03541-12

66. Kandolf R, Hofschneider PH. Molecular cloning of the genome of a cardiotropic Coxsackie B3 virus: full-length reverse-transcribed recombinant cDNA generates infectious virus in mammalian cells. *Proc Natl Acad Sci*. 2006;82(14):4818-4822. doi:10.1073/pnas.82.14.4818

67. Schneider CA, Rasband WS, Eliceiri KW. NIH Image to ImageJ: 25 years of image analysis. *Nat Methods*. 2012;9(7):671-675. http://www.ncbi.nlm.nih.gov/pubmed/22930834%0Ahttp://www.pubmedcentral.nih.gov/articlerender.fcgi?artid=PMC5554542.

68. Kilianski A, Mielech AM, Deng X, Baker SC. Assessing Activity and Inhibition of Middle East Respiratory Syndrome Coronavirus Papain-Like and 3C-Like Proteases Using Luciferase-Based Biosensors. *J Virol*. 2013;87(21):11955-11962. doi:10.1128/JVI.02105-13

69. Guo Z, Zhong X, Lin L, et al. A 3C pro -dependent bioluminescence imaging assay for in vivo evaluation of anti-enterovirus 71 agents. *Antiviral Res*. 2014;101(1):82-92. doi:10.1016/j.antiviral.2013.11.002

70. Wang L, Fu Q, Dong Y, et al. Bioluminescence imaging of Hepatitis C virus NS3/4A serine protease activity in cells and living animals. *Antiviral Res*. 2010;87(1):50-56. doi:10.1016/j.antiviral.2010.04.010

71. Blom N, Hansen J, Blaas D, Brunak S. Cleavage site analysis in picornaviral polyproteins: Discovering cellular targets by neural networks. *Protein Sci*. 1996;5(11):2203-2216. doi:10.1002/pro.5560051107

72. Lucas M, Karrer U, Lucas A, Klenerman P. Viral escape mechanisms - Escapology taught by viruses. *Int J Exp Pathol*. 2001;82(5):269-286. doi:10.1046/j.1365-2613.2001.00204.x

73. Lee CC, Kuo CJ, Ko TP, et al. Structural basis of inhibition specificities of 3C and 3C-like proteases by zinc-coordinating and peptidomimetic compounds. *J Biol Chem*. 2009;284(12):7646-7655. doi:10.1074/jbc.M807947200

74. Kaur-Sawhney R, Shih L mei, Cegielska T, Galston AW. Inhibition of protease activity by polyamines. Relevance for control of leaf senescence. *FEBS Lett*. 1982;145(2):345-349. doi:10.1016/0014-5793(82)80197-X

75. Rezaei-Ghaleh N, Ebrahim-Habibi A, Moosavi-Movahedi AA, Nemat-Gorgani M. Effect of polyamines on the structure, thermal stability and 2,2,2-trifluoroethanol-induced aggregation of α-chymotrypsin. *Int J Biol Macromol*. 2007;41(5):597-604. doi:10.1016/j.ijbiomac.2007.07.018

76. Dial CN, Tate PM, Kicmal TM, Mounce BC. Coxsackievirus B3 Responds to Polyamine Depletion via Enhancement of 2A and 3C Protease Activity. *Viruses*. 2019;11(403).

VITA

The author, Courtney Dial, was born in Naperville, Illinois on December 2nd, 1994 to Robert and Jennifer Dial. She attended Lewis University in Romeoville, Illinois where she earned her Bachelor of Science degree in Biochemistry with a minor in Biology graduating from Lewis University in May 2017, *cum laude,* as a Distinguished Scholar of the University. She began her undergraduate research education in the lab of Dr. Jason J. Keleher studying novel water filtration systems. From there she moved into the lab of Dr. Sarah E. Powers investigating the role of cyclin D3 and its correlation to cancer. After graduation, she matriculated to Loyola University Chicago, in July 2017, in the Infectious Disease and Immunology Master's program under the mentorship of Dr. Bryan C. Mounce.

Courtney's thesis work focused on determining the role polyamines play in viral proteolytic activity as well as RNA virus evolution. After completion of her Master of Science degree, Courtney will continue her training in the IPBS program at Loyola University Chicago, Stritch School of Medicine.